Orexin neurons are indispensable for prostaglandin E_2-induced fever and defence against environmental cooling in mice

Running title: Orexin neurons in PGE_2 and cooling-induced thermogenesis

Yoshiko Takahashi[1,2], Wei Zhang[3], Kohei Sameshima[1], Chiharu Kuroki[1,2], Ami Matsumoto[1], Jinko Sunanaga[1,2], Yu Kono[1], Takeshi Sakurai[4], Yuichi Kanmura[2], and Tomoyuki Kuwaki[1]

Departments of [1]Physiology and [2]Anesthesiology & Critical Care Medicine, Kagoshima University Graduate School of Medical & Dental Sciences, Kagoshima 890-8544, Japan;
[3]Department of Surgery, University of Alabama at Birmingham, Birmingham 35294-0007, AL, U.S.A.;
[4]Department of Molecular Neuroscience and Integrative Physiology, Graduate School of Medical Science, Kanazawa University, Ishikawa 920-8640, Japan

Corresponding Author: Tomoyuki Kuwaki, Ph. D.
Department of Physiology, Kagoshima University Graduate School of Medical and Dental Sciences, Sakuragaoka 8-35-1, Kagoshima 890-8544, Japan.
Phone: +81-99-275-5227, Fax: +81-99-275-5231
E-mail: kuwaki@m3.kufm.kagoshima-u.ac.jp

Keywords: Prostaglandin E; brown adipocyte; Hypocretin

Total number of words (excluding references and figure legends): 7,622

Key points

•We recently showed that orexin neurons in the hypothalamus are indispensable for stress-induced thermogenesis.

•In this study we examined whether the orexin neurons are also important for other forms of thermogenic processes, including brain PGE_2 injection that mimics inflammatory fever and environmental cold exposure.

•As was the case with stress-induced thermogenesis, orexin neuron ablated (ORX-AB) mice exhibited a blunted PGE_2-induced fever and intolerance to cold (5°C) exposure.

•Injection of retrograde tracer into the medullary raphe nucleus, where sympathetic premotor neurons regulating thermogenesis by the brown adipose tissue are located, revealed direct and indirect projection from the orexin neurons, of which the latter seemed to be preserved in the ORX-AB mice.

•These results suggest that orexin neurons are important in general thermogenic processes, and their importance is not restricted to stress-induced thermogenesis.

Word count: 131

Abstract

We recently showed using prepro-orexin knockout (ORX-KO) mice and orexin neuron-ablated (ORX-AB) mice that orexin neurons in the hypothalamus, but not orexin peptides *per se*, are indispensable for stress-induced thermogenesis. In order to examine whether orexin neurons are more generally involved in central thermoregulatory mechanisms or not, we applied other forms of thermogenic perturbations, including brain PGE_2 injections which mimic inflammatory fever and environmental cold exposure, to ORX-KO mice, ORX-AB mice, and their wild-type (WT) litter mates. We found that ORX-AB mice, but not ORX-KO mice, exhibited a blunted PGE_2-induced fever and intolerance to cold (5°C) exposure, and these findings were similar to the results previously obtained with stress-induced thermogenesis. PGE_2-induced shivering was also attenuated in ORX-AB mice. Both mutants responded similarly to environmental heating (39°C). In WT and ORX-KO mice, the administration of PGE_2 and cold exposure activated orexin neurons, as revealed by increased levels of expression of c-fos. Injection of retrograde tracer into the medullary raphe nucleus revealed direct and indirect projection from the orexin neurons, of which the latter seemed to be preserved in the ORX-AB mice. In addition, we found that glutamate receptor antagonists (D-(-)-2-amino-5-phosphonopentanoic acid and 6-cyano-7-nitroquinoxaline-2,3-dione) but not orexin receptor antagonists (SB334867 and OX2 29) successfully inhibited PGE_2-induced fever in WT mice. These results suggest that orexin neurons are important in general thermogenic processes, and their importance is not restricted to stress-induced thermogenesis. In addition, these results indicate the possible involvement of glutamate in orexin neurons implicated in PGE_2-induced fever.

Abbreviations

AP5, D-(-)-2-amino-5-phosphonopentanoic acid; AUC, area under the curve; BAT, brown adipose tissue; CNQX, 6-cyano-7-nitroquinoxaline-2,3-dione; CTb, cholera toxin subunit b; DHA, dorsal hypothalamic area; DMH, dorsomedial hypothalamus; GFP, green fluorescent protein; LHA, lateral hypothalamic area; MPO, medial preoptic area; ORX-AB, orexin-neuron-ablated mice; ORX-KO, orexin-knockout mice; WT_{AB}, wild-type littermate of the orexin-neuron-ablated mice; WT_{KO}, wild-type littermate of the orexin knockout mice.

Introduction

Central thermoregulatory pathways are composed of multiple parallel circuits that are active depending upon the causes of the thermogenesis and the output targets [brown adipose tissue (BAT), skin blood vessels, and/or skeletal muscles] (Rathner *et al.*, 2008; Yoshida *et al.*, 2009; McAllen *et al.*, 2010; Nakamura, 2011). For example, stress-induced thermogenesis is inhibited by benzodiazepines, but not by cyclooxygenase inhibitors, while lipopolysaccharide-induced fever is inhibited by cyclooxygenase inhibitors, but not by benzodiazepines (Vinkers *et al.*, 2009). The responsiveness of tail blood vessels is more sensitive to core body cooling than to skin cooling, while the responsiveness of BAT is relatively more sensitive to skin cooling than to core cooling (McAllen *et al.*, 2010). Inactivation of the dorsomedial hypothalamus (DMH)/dorsal hypothalamic area (DHA), which is one of the major relay nuclei of central thermoregulation (Samuels *et al.*, 2004; Nakamura *et al.*, 2005; Nakamura & Morrison, 2007; Morrison, 2011; Morrison & Nakamura, 2011; Nakamura & Morrison, 2011; Tupone *et al.*, 2011), attenuates BAT thermogenesis, but not skin vasoconstriction, in response to an injection of PGE_2 into the preoptic area (Rathner *et al.*, 2008).

We recently showed using orexin-neuron-ablated (ORX-AB) mice that orexin neurons in the hypothalamus are indispensable for stress-induced thermogenesis (Zhang *et al.*, 2010). Orexin neurons are located in the lateral hypothalamic area, the perifornical area, and the DMH (Elias *et al.*, 1998; Peyron *et al.*, 1998; Nambu *et al.*, 1999), which is the thermogenic nucleus described above. However, it is currently unclear whether the orexin neurons are important for the stress-induced form of thermogenesis only or if they are more generally involved in the above-mentioned central thermoregulatory mechanisms. In order to research this question, we applied other forms of thermogenic perturbations, including PGE_2 injections and cold exposure, to ORX-AB mice. We expected that orexin neurons would have a more generalised role because some orexin neurons project to the medullary raphe (Elias *et al.*, 1998; Peyron *et al.*, 1998; Nambu *et al.*, 1999), which is a site where all of the thermogenic output pathways to the BAT, blood vessels, and skeletal muscles make synaptic connections (McAllen *et al.*, 2010). In addition, orexin neurons regulate the sleep/wake state (Sakurai, 2007) and, thus, they may affect body temperature regulation in a general way.

In addition, our previous study (Zhang *et al.*, 2010) showed relatively

surprising results. Stress-induced thermogenesis was attenuated in ORX-AB mice, but not in orexin knockout (ORX-KO) mice, which lack orexin but have preserved co-localised neurotransmitter/modulator candidates, such as glutamate (Abrahamson *et al.*, 2001; Rosin *et al.*, 2003; Torrealba *et al.*, 2003), dynorphin (Chou *et al.*, 2001), galanin (Hakansson *et al.*, 1999), and nitric oxide (Cheng *et al.*, 2003) in the orexin neurons. These results indicated the importance of the co-localised substances in the orexin neurons but not of orexin *per se* in stress-induced thermogenesis. In fact, the existence of orexin-dependent and -independent forms of thermogenesis has recently been proposed (Rusyniak *et al.*, 2011). Dynorphin and glutamate may act synergistically with orexin in order to promote wakefulness (Arrigoni *et al.*, 2010). Nevertheless, the precise role(s) of the substances co-localised with orexin are largely unknown.

The aim of the present study was to examine whether orexin and the substances co-localised in orexin neurons contribute to PGE_2-induced fever and cold defence. We hypothesised that ORX-AB mice, but not ORX-KO mice, would show attenuation of PGE_2-induced fever and cold tolerance, as was seen for handling stress-induced thermogenesis (Zhang *et al.*, 2010). In addition, we examined the possible effects of pre-treatment with orexin receptor antagonists and glutamate receptor antagonists in PGE_2-induced fever in wild-type (WT) mice. We found, as expected, that ORX-AB, but not ORX-KO mice, have blunted PGE_2-induced febrile responses and intolerance to cold exposure. In addition, we found that glutamate receptor antagonists, but not orexin receptor antagonists, successfully inhibited PGE_2-induced fever. These results show the generalised importance of orexin neurons in thermogenesis, and their importance is not restricted to stress-induced one. In addition, these results indicate the possible importance of glutamate in orexin neurons that are involved in PGE_2-induced fever.

Methods

Ethical approval

All experimental procedures were performed in accordance with the guiding principles for the care and use of animals in the field of physiological sciences published by the Physiological Society of Japan (2003) and approved by the Institutional Animal Use Committee at Kagoshima University.

Animals

Animals used in this study were 5- to 8-month-old male ORX-KO mice, ORX-AB mice, and corresponding WT littermates (WT_{KO} and WT_{AB}). The ORX-KO mice, which have a nuclear translocation signal plus the LacZ (also known as β-galactosidase) gene inserted into the prepro-orexin gene, do not produce orexin-A and -B (Chemelli *et al.*, 1999). ORX-KO mice were maintained as heterozygotes and crossed in order to obtain null mutants and WT_{KO} mice. In ORX-AB mice, almost all (>98%) of the orexin neurons were ablated by 4 months of age through the expression of the neurotoxin, ataxin-3, under the control of the human orexin promoter (Hara *et al.*, 2001). Thus, comparing the phenotypes of ORX-KO mice and ORX-AB mice allow us to test the roles of other neurotransmitters (e.g. glutamate and dynorphin) that are produced in orexin neurons (Chou *et al.*, 2001; Rosin *et al.*, 2003). ORX-AB mice were also maintained as heterozygotes and crossed with C57BL/6 (Clea Japan Inc., Tokyo, Japan) in order to obtain ORX-AB mice and WT_{AB}. In order to maximise genetic homogeneity, we backcrossed the ORX-KO and ORX-AB mice with C57BL/6 for more than 10 generations. The genotypes of ORX-KO and ORX-AB mice were identified by PCR of DNA extracted from the tail, as has been previously reported (Terada *et al.*, 2008; Zhang *et al.*, 2009).

In an immunohistochemical experiment (see below), we used ORX-KO;ORX-green fluorescent protein (GFP) mice, which were the offspring from a crossing of ORX-KO mice and ORX-GFP mice. The latter expressed enhanced GFP exclusively in orexin neurons, which were under the control of the human orexin promoter (Yamanaka *et al.*, 2003). ORX-KO;ORX-GFP mice do not produce orexin-A and -B but efficiently express GFP in orexin neurons. We used ORX-KO;ORX-GFP mice because the anti-LacZ staining in ORX-KO mice in our previous study (Zhang *et al.*,

2010) revealed a low penetration rate (~10%) of LacZ in orexin neurons because of an unknown reason. Enzymatic staining with X-Gal as a substrate also revealed a low penetration rate in ORX-KO mice (unpublished observation).

All mice were housed in a room that was maintained at 22–24°C and with lights on at 7:00 AM and off at 7:00 PM. Mice had food and tap water available *ad libitum*. All of the animal experiments were performed in a quiet and air-conditioned (22–24°C) room from 11:00-17:00 in order to avoid any possible influences of circadian rhythms on body temperature.

Measurement of BAT, rectal temperatures and muscle movements under anaesthesia

Mice were anaesthetised with an i.p. injection of a mixture of α-chloralose (80 $mg \cdot kg^{-1}$) and urethane (800 $mg \cdot kg^{-1}$). The adequacy of the anaesthesia was judged by the absence of the withdrawal reflex to a pinching stimulus. The animals were warmed with a heating pad (set at 33°C), and they were allowed to breath spontaneously. The animals were placed in a prone position in a stereotaxic frame (ST-7, Narishige Scientific Instrument Lab, Tokyo, Japan) so that Bregma and Lambda were on a horizontal plane. A small hole was drilled in the skull through which a glass micropipette or a microsyringe was inserted into the brain.

A thermo probe (IT-23, Physitemp Instruments, Inc., Clifton, NJ, USA) was implanted in the BAT, and the skin was sutured. Another thermo probe (RET-3) was inserted into the rectum. An EMG was obtained from pin electrodes attached to the nuchal muscles. After completion of the surgery, at least 1 h was allowed to pass in order for the variables to stabilise.

The EMG signals were amplified (×10,000, AVB-21, Nihon Kohden Corporation, Tokyo, Japan) with band-pass filters (50–1,000 Hz) and fed into a personal computer after analog-to-digital conversion (PowerLab, ADInstruments Pty Ltd., Bella Vista, NSW, Australia) at a sampling frequency of 4,000 Hz. The EMG signals were full-wave rectified, leak integrated (time constant = 0.1 s), and standardised with the baseline value from each individual animal.

Microinjection of PGE_2 into the Medial Preoptic Area

The methods used for the microinjection of drugs into the brain and the verification of the injection sites were the same as those in our previous reports (Kayaba *et al.*, 2003; Zhang *et al.*, 2006; Zhang *et al.*, 2009). In brief, the glass micropipette (outside tip diameter of 20–30 μm) was attached to a stereotaxic micromanipulator and connected by silicon tubing to a pressure injector (IM-200J, Narishige Scientific Instrument Lab). The tip of the pipette was positioned at 0.0 mm anteroposterior to the Bregma, 0.3 mm lateral to the midline, and 4.9 mm ventral to the surface of the skull. While observing the fluid meniscus in the micropipette through a dissection microscope that was equipped with an ocular micrometre, a volume of 20 nL was injected by adjusting the pressure and time of the injection.

After 10 min of control recordings, ACSF and PGE_2 (1 $mg \cdot mL^{-1}$ dissolved in ACSF) were sequentially administered in this order with an interval of 90 min. At the end of the experiment, the injection site was marked by injecting 20 nL of a 4% Evans blue solution through another micropipette. The animal was deeply anaesthetised with additional chloralose/urethane and transcardially perfused with 20 mL of heparin-added saline, which was followed by 20 mL of 4% formalin. The brains were removed and stored in the formalin solution for at least 2 days before sectioning. Coronal sections of 50-μm thickness were cut serially with a vibrating microslicer (D.S.K. supermicroslicer, Dosaka EM, Kyoto, Japan), mounted on adhesive-coated slides (Frontier, Matsunami Glass Ind., Ltd., Osaka, Japan), and stained with 1% neutral red. The locations of the injection sites were determined according to the atlas of Paxinos & Franklin (2001).

Telemetric measurement of body temperature

With a telemetric system (Dataquest, Data Sciences International, St. Paul, MN, USA), we measured abdominal temperature and locomotor activity in a freely moving mouse in his home cage. At least 7 days before the experiment, a telemetric device (TA10ETA-F10, Data Sciences International) was implanted in the abdominal cavities of mice while they were under anaesthesia with 2–3% isoflurane. Also implanted was a guide cannula (C315GS-5/2.5; Plastics One Inc., Roanoke, VA, USA) for the intracerebroventricular administration of drugs to the lateral ventricle (1 mm lateral to the Bregma, 2.5 mm deep in the skull) (Deng *et al.*, 2007). The guide cannula was closed with a cannula dummy cap and firmly fixed to the skull with dental cement. An antibiotic,

cephalosporin (50 mg·kg^{-1}), was injected subcutaneously before the surgery.

After a recovery period of 1 week, PGE_2 (1 mg·mL^{-1}) or vehicle (ACSF) was administered (2 μL) into the lateral ventricle in a random order with an intermission of at least 2 days. After finishing the PGE_2/ACSF experiments, the animals were exposed to cold (5°C for 4 h) or hot (39°C for 1 h) environments in a random order with an intermission of at least 2 days. Cold and hot exposure was achieved by putting the animal's home cage into a refrigerator and an incubator, respectively. Out of 5 ORX-AB animals examined, 4 mice did not tolerate 4 h of cold exposure (see Results section). After their body temperature decreased below 30°C, these animals were taken out of the refrigerator and warmed with a heating lamp immediately.

Pharmacological experiment

We used C57BL/6 mice (Clea Japan Inc.) in this experiment. The methods for anaesthesia, stereotaxic head fixing, temperature measurement, and EMG recordings were the same as those described above. The only exception was that the trachea was cannulated with polyethylene tubing for artificial ventilation because some drugs may affect not only body temperature, but also respiration. The animals were ventilated (Mini Vent TYPE 845, Hugo Sachs Elektronik-Harvard Apparatus GmbH, March-Hugstetten, Germany) with oxygen-enriched (~50%) room air. The tidal volume and the frequency of the ventilator were set to 150–200 μL and 150–200 min^{-1}, respectively (Toyama *et al.*, 2009). After a stabilization period of 1 h or more, 2 μL of the drug to be examined was administered with a microsyringe from a drilled hole over the lateral ventricle. After 5 min, PGE_2 (1 mg·mL^{-1}, 2 μL) was administered into the same ventricle with another microsyringe, and the effects on BAT temperature, rectal temperature, and EMG were observed for another 90 min. Only 1 drug was examined in each animal.

Five drugs were examined: ACSF (pH 7.4); an orexin receptor-1 specific antagonist, SB334867 (1 mM, Tocris Bioscience, Bristol, UK); an orexin receptor-2 specific antagonist, OX2 29 (100 mM, Tocris Bioscience); a NMDA-selective glutamate receptor antagonist, D-(-)-2-amino-5-phosphonopentanoic acid (AP5, 10 mM, Sigma-Aldrich Co., St. Louis, MO, USA); and an AMPA/kainate-selective glutamate receptor antagonist, 6-cyano-7-nitroquinoxaline-2,3-dione (CNQX, 10 mM, Tocris Bioscience). All drugs were dissolved in ACSF except for SB334867. SB334867 is

hydrophobic and was initially dissolved in DMSO to a concentration of 350 mM (maximum soluble concentration), and the solution was then diluted with 45% (2-hydroxypropyl)-β-cyclodextrin (Encapsin, Sigma-Aldrich Co.) in ACSF in order to make 10 mM of SB334867. This solution was further diluted with ACSF to make 1 mM of SB334867. In our preliminary study, neither the vehicle (4.4% Encapsin-0.3% DMSO in ACSF) nor 0.3% DMSO in ACSF affected the successive PGE_2-induced increase in BAT temperature, while 1% DMSO did. Therefore, 1 mM was the maximum concentration of SB334867 used in the current experimental setup.

Immunohistochemistry

The activation of orexin neurons by intracerebroventricular injections of PGE_2 or by cold exposure was examined by double immunohistochemical staining for orexin and c-fos using method that were similar to those previously reported but with minor modifications (Watanabe *et al.*, 2005; Sunanaga *et al.*, 2009; Zhang *et al.*, 2009; Zhang *et al.*, 2010). In brief, 2 h after the PGE_2 or ACSF injections or 1 h after the cold exposure (some ORX-AB mice did not tolerate longer cold exposures, see Results section), the mice were deeply anaesthetised by an i.p. injection of urethane (1.6 $g \cdot kg^{-1}$) and transcardially perfused with 10 mM PBS, which was followed by a fixative solution containing 4% paraformaldehyde in PBS. Brains were excised and post-fixed in the same fixative solution for 48 h at 4°C. As a control for the cold exposure, brains obtained from naïve mice were also used. After cryoprotection with 30% sucrose, serial transverse frozen sections (40 μm) were cut from the brain tissue that included the hypothalamus. Every fourth section was collected and sequentially incubated with PBS containing 0.3% Triton-X and 1% normal donkey serum for 30 min, rabbit anti-c-fos antiserum (1:1,000, PC-38, Merck KGaA, Darmstadt, Germany) for 1 h, biotinylated goat anti-rabbit IgG antibody (1:200, Vector Laboratories, Inc., Burlingame, CA, USA) for 1 h, and goat anti-orexin antiserum (1:100, sc-8070, Santa Cruz Biotechnology, Inc., Santa Cruz, CA, USA) for 1 h at room temperature. Finally, the tissue was incubated with Alexa Fluor 488 streptavidin conjugate (1:200, Invitrogen Corporation, Carlsbad, CA, USA) and Alexa Fluor 568-labeled donkey anti-goat IgG antibody (1:200, Invitrogen) for 90 min in a dark box. The sections were then mounted on glass slides, coverslipped using mounting medium with or without DAPI (Vector Laboratories), and examined with a fluorescence

microscope (Biorevo BZ-8000, Keyence Corporation, Osaka, Japan and LSM700, Carl Zeiss Japan, Tokyo, Japan). Images were recorded with a 48-bit digital camera (1020 x 1350 μm window). In order to confirm the specificity of the antibodies, sections that were incubated without primary or secondary antibody were used as negative controls for each experiment, and no signals were observed.

For ORX-KO mice that did not express orexin, we used ORX-KO;ORX-GFP mice (see *Animals*). Brain sections were prepared by the same method described above and incubated with a rabbit anti-c-fos antiserum. A biotin-streptavidin system was not used. Instead, an Alexa Fluor 568-labeled goat anti-rabbit IgG antibody (1:200, Invitrogen Corporation) was used.

The numbers of single-labelled (c-fos or orexin) and double-labelled (orexin plus c-fos) cells were counted on a computer screen with an assistance of count tool in Adobe Photoshop software by an experimenter who did not know the treatment (PGE_2/ACSF or cold/naïve). Every 4th section in an animal (6 sections per mouse) was examined, since orexin neurons were distributed over a rostral-caudal distance of ~1 mm (Sakurai *et al.*, 1998). Several reports have proposed functional dichotomy of orexin neurons located in the lateral hypothalamus and those in perifornical/dorsomedial hypothalamic area (Estabrooke *et al.*, 2001; Fadel *et al.*, 2002; Harris *et al.*, 2005; Sunanaga *et al.*, 2009; Zhang *et al.*, 2009). Therefore, immunoreactivity was separately counted for medial and lateral hypothalamic areas.

Retrograde labelling of the neurons projecting to the rostral raphe pallidus

Retrograde labelling experiment (Conte *et al.*, 2009; Tupone *et al.*, 2011) was performed to examine whether the descending neuronal pathways from the hypothalamus to the rostral raphe pallidus, a thermogenic centre in the lower brainstem (Nakamura & Morrison, 2007; Morrison, 2011; Morrison & Nakamura, 2011; Nakamura & Morrison, 2011; Tupone *et al.*, 2011), in ORX-AB mice were normally preserved or not. WT_{AB} and ORX-AB mice (n=4 each), anaesthetized with intraperitoneal injection of ketamine (100 mg/kg) and xylazine (0.5 mg/kg), were stereotaxically injected with cholera toxin subunit b (CTb, 20 mg/ml, 50 nL) conjugated to Alexa Fluor 488 (Invitrogen) into the rostral raphe pallidus (coordinate from the Bregma: 6.6 mm caudal, 0.0 mm lateral, and 6.2 mm ventral) and the pipette was left in place for 5 min. Mice were treated with analgesic (0.05 mg/kg buprenorphine, s.c.) after the drilled hole on the skull was covered with an

ointment containing antibiotic bacitracin and neomycin and the skin was sutured. After 4 days, the mice were deeply anaesthetized by an injection of urethane (1.6 $g \cdot kg^{-1}$, i.p.) and transcardially perfused with 10 mM PBS, which was followed by a fixative solution containing 4% paraformaldehyde in PBS. Brains were excised, post-fixed, cryoprotected, and thin-sectioned as described above (Immunohistochemistry section).

CTb in the hypothalamus was detected with goat anti CTb antiserum (1:1,000, List Biological, Campbell, CA, USA), biotinylated horse anti-goat IgG antibody (1:200, Vector Laboratories), and Alexa Fluor 488 streptavidin conjugate. CTb in the brainstem was detected by fluorescence of Alexa Fluor 488 conjugated to CTb without immunostaining. Orexin was labeled with rabbit anti orexin antiserum (1:1,000, Peptide Institute, Osaka, Japan) and Alexa 568-conjugated goat anti-rabbit IgG antibody (1:200, Vector Laboratories).

BAT morphology

To examine whether the BAT in the mutant mice was normal or not, microscopic morphology of the BAT was studied in WT_{KO}, ORX-KO, and ORX-AB mice (n=4 each). Intrascapular BAT was dissected after decapitation, fixed in formalin, embedded in paraffin, and thin sectioned at 4 μm. Specimens were stained with haematoxylin and eosin.

Statistics

Physiological and pharmacological experimental results were assessed by ANOVA with genotype and drug as the main factor and time as a repeated measure. When appropriate, the within-subjects effects over time were determined by a Bonferroni's post hoc test. Response magnitude in each parameter over the time course was calculated as the area under the curve (AUC) above the baseline. To compare AUC among the groups, we used one-way ANOVA followed by Bonferroni's post hoc test. The immunohistochemical results were analysed by one-way ANOVA. GraphPad Prism software (GraphPad Software, Inc., La Jolla, CA, USA) was used for these calculations. Data are presented as mean ± SEM. Differences with p values less than 0.05 were considered significant.

Results

Eliminated PGE_2-induced fever in ORX-AB mice but not in ORX-KO mice

We previously showed that stress-induced thermogenesis was significantly attenuated in ORX-AB mice but not in ORX-KO mice (Zhang *et al.*, 2010). Here, we examined whether the same was true for PGE_2-induced fever, which is a different form of thermogenic response.

There were no differences in the initial BAT temperatures or rectal temperatures among the genotypes while under chloralose/urethane anaesthesia. In WT_{KO} and WT_{AB} mice, the BAT temperature increased by ~3.0°C (Fig. 1A), and the rectal temperature increased by ~1.5°C (Fig. 1B) 30 min after a microinjection of PGE_2 (20 ng, ~57 pmol) into the medial preoptic area. BAT and rectal temperatures returned almost to the initial values within 70 min.

As was the case for handling stress-induced thermogenesis in our previous study, ORX-KO mice, but not ORX-AB mice, showed similar febrile responses to those in the control mice. ORX-AB mice showed no febrile response ($p = 0.44$ for BAT and $p = 0.08$ for rectum, comparison among time points by 1-way ANOVA), and, thus, their BAT and rectal temperatures stayed within the range of the vehicle injection (Fig. 1A' and B').

In addition, we analysed nuchal EMG as a measure of shivering. Changes in the integrated EMG by PGE_2 in WT_{KO} and WT_{AB} mice peaked earlier (Fig. 1C, 10–20 min after the injection) than the changes in the BAT temperature and rectal temperature (30–40 min) and gradually returned to baseline values. In ORX-KO mice, changes in the integrated EMG occurred slowly (peaking 30 min after the injection), and the magnitude was smaller than that in WT_{KO} ($p<0.05$, Fig. 1C'). In a similar manner, changes in the integrated EMG in ORX-AB mice occurred slowly and the magnitude was smaller than that in WT_{AB} ($p<0.01$). As a whole, the PGE_2-induced responses were slightly blunted in ORX-KO mice and severely attenuated in ORX-AB mice.

The microinjection sites were examined after the experiment, and they were confirmed to be within the medial preoptic area (Fig. 1D and E).

Blunted PGE_2-induced fever in unanesthetized ORX-AB mice

In order to exclude any possible interactions with the anaesthetics in the previous experiment, we used telemetric body temperature measurements in

unanesthetized freely moving animals for the next step.

There was no difference in the initial abdominal temperature (~36.5°C) among the genotypes, although it was higher than the rectal temperatures in chloralose/urethane-anaesthetised conditions (~36.0°C). In WT_{KO} and WT_{AB} mice, the abdominal temperature increased by ~3.0°C (Fig. 2A) at 30–40 min after an injection of PGE_2 (2 μg) into the lateral ventricle. Their abdominal temperature then gradually returned to the initial values over the observation period of 150 min. In ORX-KO mice, a response that was similar to those in WT_{KO} and WT_{AB} mice was observed. In ORX-AB mice, in contrast, abdominal temperature did not change after an injection of PGE_2. Although there were some perturbations in abdominal temperature, they were not significantly different from the baseline values and not different from those after vehicle injection (Fig. 2B). Thus, the PGE_2-evoked febrile response was eliminated in ORX-AB mice, but not in ORX-KO mice, in both anaesthetised and unanesthetized conditions.

Intolerance of ORX-AB mice to environmental cooling

We next examined another type of stimulation that induces thermogenesis. Mice with indwelling telemeters were put into a cold (5°C) environment. In WT_{KO} and WT_{AB} mice, the abdominal temperature initially decreased, reached its nadir (~34°C) at around 90 min, and then slightly increased towards the baseline (Fig. 3A). Although the abdominal temperatures never returned to the initial value during the cold exposure, it remained over 34°C and returned to the initial value after the animals were returned to room temperature (22–24°C).

In ORX-KO mice, a similar change in abdominal temperature was observed in comparison with those in WT_{KO} and WT_{AB} mice. However, 4 out of 5 ORX-AB mice did not tolerate 4 h of cold exposure. In particular, in 3 ORX-AB mice, abdominal temperature rapidly fell and reached the endpoint of 30°C within 50–150 min of cold exposure. The magnitude of the temperature decrease in ORX-AB mice was significantly greater ($p<0.05$) than that in WT_{AB} mice when evaluated as AUC during the initial 60 min (inset of the Fig. 3A).

In the cold-exposure experiment, we also analysed locomotor activity of the mice (Fig. 3B). Locomotion was increased in only the initial period of less than 30 min, and, thereafter, all of the mice stayed in one place in a crouching position and surrounded

by wooden bedding chips. There was no difference in locomotor activity among the genotypes (inset of the Fig. 3B). Therefore, the intolerance of the ORX-AB mice to the cold exposure cannot be explained by a defect in behavioural thermoregulation in this mutant.

Preserved response to hot exposure in ORX-AB mice

In order to further examine the temperature regulation in ORX-AB mice, the animals were exposed to a hot environment (39°C). In WT_{KO} and WT_{AB} mice, the abdominal temperature increased by ~1.5°C 40 min after the heat exposure and remained at the highest value (~38°C) during the latter half of the exposure period (Fig. 4A). After the animals were returned to a room temperature (22–24°C) environment, abdominal temperature soon returned to the baseline and fell further below the baseline. Locomotor activity significantly increased for the initial 10 min and gradually returned to the baseline value during the entire exposure period (Fig. 4B).

In ORX-KO and ORX-AB mice, the changes in abdominal temperature and changes in locomotor activity in response to heat exposure compared to controls were identical with respect to the time course and the magnitude.

Activation of hypothalamic neurons by PGE_2 and cold exposure

We next examined whether the orexin neurons and other hypothalamic neurons were activated by the intracerebroventricular administration of PGE_2 or by cold exposure. For this purpose, we performed the immunohistochemical detection of orexin-like (in the WT_{AB} mice and the ORX-AB mice) immunoreactivity together with that of c-fos-like immunoreactivity. In addition, we used ORX-KO;ORX-GFP mice (see *Animals* section for details). ORX-KO;ORX-GFP mice do not produce orexin-A and -B but efficiently and exclusively express GFP in orexin neurons. In our preliminary study, in fact, a ORX-KO heterozygous mouse which carried the ORX-GFP transgene expressed GFP in ~80% of orexin-immunopositive cells, and the ectopic expression of GFP was never observed, as was the case in WT;ORX-GFP mice (Yamanaka *et al.*, 2003). An ORX-KO;ORX-GFP mouse did not show any orexin-like immunoreactivity, as expected.

After the administration of PGE_2 in WT_{AB} mice, the numbers of c-fos-immunopositive cells and double-labelled (orexin plus c-fos) cells in both medial

and lateral hypothalamic areas (Fig. 5E) were significantly larger than those observed after vehicle administration, while the total number of orexin-immunopositive cells was not different between the treatments (Fig. 5F, G). Consequently, the percentage of double-labelled cells among the orexin-positive cells was significantly higher in the brains of PGE_2-treated WT_{AB} mice (66.4 ± 11.7% in the medial area and 37.8 ± 7.2% in the lateral area, n = 4) than in vehicle-treated WT_{AB} mice (23.7 ± 7.1% in the medial area and 18.9 ± 2.4% in the lateral area, n = 4, $p < 0.05$).

In the ORX-KO;ORX-GFP mice, a similar result was obtained (double-labelled cells were 73.9 ± 8.2% and 44.1 ± 8.2% in the medial and lateral hypothalamic areas, respectively, with PGE_2 treatment, n = 4 vs. 26.5 ± 2.3% and 23.1 ± 1.9% in the medial and lateral hypothalamic areas, respectively, with vehicle treatment, n = 4, $p < 0.05$), although there was no difference in the total numbers of GFP-positive and orexin-immunopositive cells in WT_{AB} mice.

No orexin-like immunoreactivity was observed in the ORX-AB mice, as expected. Of note, the numbers of c-fos-positive cells were not increased by PGE_2-treatment in the medial hypothalamic area (Fig. 5F) while comparable increase was observed in the lateral hypothalamic area (Fig. 5G).

In order to examine the possible activation of orexin neurons by cold exposure, we used untreated naïve mice as the controls, and experimental brains were excised after 1 h of cold exposure. There was no difference in the total number of orexin-immunopositive cells (~220 in the medial hypothalamic area and ~280 in the lateral hypothalamic area) in WT_{AB} mice and GFP-positive cells (~200 in the medial hypothalamic area and ~240 in the lateral hypothalamic area) in ORX-KO;ORX-GFP mice between the cold exposure experiment (Fig. 6) and the PGE_2 experiment (Fig. 5), showing reproducible results. As was the case with PGE_2 treatment, cold exposure increased the number of c-fos-positive cells in the areas examined in the hypothalamus in both WT_{AB} mice and ORX-KO;ORX-GFP mice. Cold exposure significantly increased the percentage of double-labelled cells among the orexin- or GFP-positive cells in both WT_{AB} mice (81.3 ± 4.0% and 59.6 ± 8.2% in the medial and lateral hypothalamic areas, respectively, n = 4 with cold exposure vs. 23.6 ± 5.1% and 17.7 ± 4.0% in the medial and lateral hypothalamic areas, respectively, n = 4 in the controls, $p < 0.01$) and ORX-KO;ORX-GFP mice (65.0 ± 7.1% and 52.8 ± 4.2% in the medial and lateral

hypothalamic areas, respectively, n = 4 with cold exposure vs. 17.6 ± 3.9% and 24.2 ± 5.2% in the medial and lateral hypothalamic areas, respectively, n = 4 in the controls, $p < 0.01$).

In the ORX-AB mice, no orexin-like immunoreactivity was observed. Cold exposure increased c-fos expression in the lateral hypothalamic area but not in the medial hypothalamic area (Fig. 6), which was similar to the PGE_2-experiment (Fig. 5).

The number of c-fos-positive cells in the control naïve mice brains (100–200, Fig. 6) in the cold exposure experiment was far fewer than that in the vehicle-treated control mice brains in the PGE_2-experiment (400–500, Fig. 5). These results showed that injections of vehicle were somewhat stressful. However, it should be emphasized that injection of PGE_2 further increased c-fos positive cells and double-labelled cells.

Preserved descending pathway from the hypothalamus to medullary raphe nucleus in ORX-AB mice

In order to examine whether the descending neuronal pathways from the hypothalamus to the rostral raphe pallidus in ORX-AB mice were normally preserved or not, we performed retrograde labelling experiment. Four days after injection of CTb into the raphe pallidus (Fig. 7B, E), CTb-immunopositive cells were found in the dorsal, medial, and lateral regions of the hypothalamus (Fig. 7A, D). In WT_{AB} mice, the distribution of CTb-positive cells in the LHA, perifornical area, and lateral part of the DMH overlaps with the distribution of orexin neurons and many of the CTb-positive cells also expressed orexin. Outside of the distribution area of the orexin neurons, there was a cluster of CTb-positive cells in medial part of the DMH near the third ventricle and the DHA. Of note, some of the CTb-positive cells in the DHA seemed to be innervated by orexin-containing nerve terminals (Fig. 7C').

Although orexin neurons were completely disappeared in ORX-AB mice, there was no difference in the number (690 ± 46 in WT_{AB} vs. 653 ± 48 in ORX-AB, n=4 each) or distribution of the CTb-positive cells within the hypothalamus as compared to the WT_{AB} mice. Of note, a cluster of CTb-positive cells in DMH/DHA was well preserved.

Preserved BAT morphology in ORX-AB mice

To examine whether the BAT in the mutant mice was normal or not,

microscopic morphology of the BAT was studied in WT_{KO}, ORX-KO, and ORX-AB mice (n=4 each). Intrascapular BAT was apparently normal in both ORX-KO and ORX-AB mice (Fig. 8), indicating that abnormal thermoregulation in ORX-AB cannot be attributed to abnormality of the BAT.

Attenuation of PGE_2-induced fever by glutamate, but not orexin, blockers

In order to further examine the possible neurotransmitters that are involved in PGE_2-induced fever, we conducted a pharmacological experiment using WT mice of the C57BL/6 strain.

In chloralose/urethane-anaesthetised mice, intracerebroventricular injections of PGE_2 (2 μg) increased the BAT temperature (Fig. 9A and 9A') and rectal temperature (Fig. 9B and 9B'), as was the case in unanesthetized mice with indwelling telemeters. Increases in the temperature in this experiment (BAT by ~2°C and rectum by ~1°C) were, however, smaller than those in the unanesthetized condition (by ~3°C, see Fig. 2). Pre-treatment (icv) with an orexin-1 receptor antagonist, SB334867 (2 μmol), or with an orexin-2 receptor antagonist, OX2 29 (200 μmol), did not affect the febrile effects of the subsequent injections of PGE_2. In contrast, icv pre-treatment with a NMDA-selective glutamate receptor antagonist, AP5 (20 μmol), and with an AMPA/kainate-selective glutamate receptor antagonist, CNQX (20 μmol), significantly inhibited the febrile effects of the subsequent injection of PGE_2.

In addition, we analysed nuchal EMG as a measure of shivering. In the vehicle-pre-treatment group after the administration of PGE_2, the integrated EMG rapidly increased and remained at high values during the entire observation period of 90 min (Fig. 9C). As was the case for the BAT temperature and rectal temperature, icv glutamate receptor antagonists, but not orexin receptor antagonists, significantly attenuated the increase in EMG (Fig. 9C').

Discussion

In our previous study using ORX-KO and ORX-AB mice, we demonstrated that orexin neurons, but not orexin *per se*, are indispensable for handling stress-induced thermogenesis (Zhang *et al.*, 2010). We hypothesised that the same would be true for PGE_2-induced fever and cold tolerance. As expected, ORX-AB, but not ORX-KO, mice showed an attenuated temperature change in response to the administration of PGE_2 into the medial preoptic area while mice were under chloralose/urethane-anaesthetised conditions (Fig. 1) and into the lateral ventricle while the mice were under awake and freely moving conditions (Fig. 2). The exceptional and unexpected result was that PGE_2-induced shivering was blunted not only in ORX-AB mice, but also in ORX-KO mice (Fig. 1). With cold exposure, body temperature in ORX-AB mice progressively decreased and reached 30°C, while the body temperature in ORX-KO mice and WT mice did not decrease below 33°C (Fig. 3). The responses of the body temperature to hot exposure did not differ among the 3 strains of mice (Fig. 4), indicating that ORX-AB mice had normal heat sensitivity. In both WT and ORX-KO mice, PGE_2 or cold exposure activated orexin neurons (Fig. 5, 6). In ORX-AB mice, c-fos expression in the DMH/DHA region, where many descending neurons to the raphe pallidus were located (Fig. 7), was not increased by PGE_2 or cold exposure. Absence of the projection from orexin neurons to the DMH/DHA neurons seemed to be at least one of the critical reasons of the abnormal thermogenesis in the ORX-AB mice. Pre-treatment with the glutamate receptor antagonists, AP5 and CNQX, but not with the orexin receptor antagonists, SB334867 and OX2 29, successfully inhibited PGE_2-induced fever and shivering (Fig. 9). Taken together, these observations support the notion that orexin neurons possess a generalised importance in thermogenesis that is not restricted to stress-induced one. In addition, these results indicate the orexin neurons can be one of the sources of glutamate transmission (Li *et al.*, 2002; Schöne *et al.*, 2012) in the DMH/DHA and in the raphe pallidus that is required for febrile and cold-evoked thermogenesis (Madden & Morrison, 2004; Cao & Morrison, 2006; Morrison, 2011; Morrison & Nakamura, 2011; Nakamura & Morrison, 2011).

Shivering and behavioural adjustments

In addition to body temperature and BAT temperature, we measured shivering

in the anaesthetised experiments (Fig. 1 and 7) and locomotor activity in unanesthetized freely moving experiments (Fig. 3 and 4). Although orexin neurons, but not orexin, seemed to be involved in BAT thermogenesis and cold tolerance, orexin *per se* may be involved in PGE_2-induced shivering because an increase in nuchal EMG was significantly attenuated not only in ORX-AB mice, but also in ORX-KO mice (Fig. 1C'). However, this possibility was not confirmed by the pharmacological experiment in which orexin receptor antagonists (SB334867 and OX2 29) did not affect shivering induced by successive intracerebroventricular injections of PGE_2. We do not know at present the reason for this apparent discrepancy. The limitations of the drug dosing (1 mM was the maximal concentration for SB33467 in the current experimental setup) and/or limited drug distribution in the brain might cause a negative result. These orexin receptor antagonists may not effective blockers, as suggested by Tupone *et at.* (2011). Differences in the PGE2 injection methods and/or the absence/presence of artificial ventilation might also affect the result. Nevertheless, we can say that orexin neurons are important for PGE_2-induced shivering, in addition to BAT thermogenesis, although we do not yet know the precise neurotransmitters involved.

In addition to internal thermogenic mechanisms, we expected possible differences in the behavioural adjustments to cold environments between ORX-AB and WT mice because basal locomotor activity is smaller in ORX-AB than in WT mice, even in a normal-room-temperature environment (Hara *et al.*, 2001). However, the increase in locomotor activity in ORX-AB mice in response to cold exposure was similar to that in WT mice. Therefore, we conclude that cold intolerance in ORX-AB mice is not due to their behavioural differences to cold exposure.

Methodological considerations in the histological experiment

In order to identify orexin neurons in orexin-deficient mice, we used anti-LacZ immunostaining in our previous study, but the sensitivity of this method was relatively low (~10% of orexin neurons were positive for LacZ) (Zhang *et al.*, 2010). Therefore, we used ORX-KO;ORX-GFP mice instead of ORX-KO mice in this study. They were the offspring from the crossing of ORX-KO mice and ORX-GFP mice, of which the latter express enhanced GFP exclusively in orexin neurons under the control of the human orexin promoter (Yamanaka *et al.*, 2003). As expected, we found ~400 GFP-positive cells

in the hypothalamus of the ORX-KO;ORX-GFP mice, which corresponds to about 80% of orexin neurons in the WT mice (~500/mouse). In addition, an ORX-KO heterozygous mouse, which carried the ORX-GFP transgene, expressed GFP in 78% (384/495) of orexin-immunopositive cells. ORX-KO;ORX-GFP mice showed no orexin-like immunoreactivity. Importantly, ORX-KO;ORX-GFP mice showed a similar phenotype to that seen in ORX-KO mice. The rectal temperature in the ORX-KO;ORX-GFP mice increased by 3.7 ± 0.3°C (n = 4) at 30 min after the intracerebroventricular injection of PGE_2. This value corresponds well to the 3.5 ± 0.2°C (n = 8) found in ORX-KO mice (Fig. 2), although the rectal temperature in the histological experiment was obtained by a spot measurement using a rectal temperature probe, while the body temperature in ORX-KO mice was continuously measured by an indwelling telemeter. Therefore, we conclude that ORX-KO;ORX-GFP mice are good substitutes for ORX-KO mice, and they allow for the reliable and easy identification of orexin neurons.

Possible reason for abnormal thermoregulation in ORX-AB mice

BAT morphology in ORX-KO mice and ORX-AB mice was normal in this study (Fig. 8). Although Sellayah *et al.* (Sellayah *et al.*, 2011) reported malformation of the BAT in ORX-KO mice, they used ORX-KO homozygous mother to make ORX-KO pups and showed that maternal orexin injections during pregnancy rescued the defect. We used ORX-KO heterozygous parents to make ORX-KO homozygous pups and WT mother to make ORX-AB transgenic mice. Therefore, there is no discrepancy between the reports. In addition, we have previously shown that pharmacologic activation with a ß3-agonist, CL316243, resulted in a normal increase of BAT temperature in both ORX-KO mice and ORX-AB mice (Zhang *et al.*, 2010). Therefore, abnormal thermoregulation in ORX-AB mice is probably attributable to abnormalities in the brain.

The thermoregulatory system in the brain can be divided into sensory and motor output pathways. Since c-fos expression in the lateral hypothalamic area of the ORX-AB mice was comparable to those in WT mice (Figs. 5 and 6), sensory input to the hypothalamus seemed not largely diminished. These results and consideration pointed out probable participation of orexin neurons in the thermogenic output pathways.

Location of the orexin neurons in the thermoregulatory circuit

There seemed to be 2 possibilities for the location of the orexin neurons in the PGE_2- and cold exposure-induced thermogenic pathways. One possibility is that some of the orexin neurons *per se* function as a part of DMH/DHA-raphe thermogenic neurons (Oldfield *et al.*, 2002; Cano *et al.*, 2003; Berthoud *et al.*, 2005; DiMicco & Zaretsky, 2007; Tupone *et al.*, 2011). Actually, some of orexin neurons located in the DMH and perifornical/LHA regions send descending projection to the raphe pallidus in rats (Tupone *et al.*, 2011) and mice (Fig 7 in this experiment). Although we expected a decreased number of CTb-positive cells in the ORX-AB mice, it was comparable to that in the WT mice. One possible explanation is that the number of CTb- and orexin-double positive cells (~60/mouse) was so small that we might not be able to detect a possible change in the whole CTb-positive population (~700). In addition, compensatory changes may occur in the ORX-AB mice.

Another possibility is that some orexin neurons provide tonic excitation to the DMH/DHA-raphe thermogenic neurons through their projection to the DMH/DHA (Peyron *et al.*, 1998). We confirmed that orexin-containing nerve terminals make apposition to some CTb-positive (having putative descending projection to in the raphe pallidus) DHA neurons (Fig 7C'). When tonic inhibition from the preoptic area to the DMH/DHA is disinhibited by cold exposure or PGE_2 (Rathner *et al.*, 2008; Yoshida *et al.*, 2009; McAllen *et al.*, 2010), this orexin neuron-dependent tonic excitation then becomes apparent in the DMH/DHA neurons. We admit, however, that orexin neurons are not the sole tonic excitatory source to the DMH/DHA-raphe thermogenic neurons because PGE_2-induced fever occurs even in the day (resting period of nocturnal mice) or under anaesthetised conditions, both of which are known to diminish spontaneous activity of the orexin neurons (Mileykovskiy *et al.*, 2005; Takahashi *et al.*, 2008). It is of interest to note, however, that the application of the same dose of PGE_2 through the same injection route induced a larger temperature increase when the animals were awake (Fig. 2) than when they are anaesthetised (Fig. 9). This observation coincides well with the above-mentioned orexin neuron-dependent tonic excitatory hypothesis.

Both the direct projection to the raphe pallidus and the indirect projection through DMH/DHA from orexin neurons were eliminated in ORX-AB mice. We cannot estimate relative importance of these pathways from current results. However, it should

be emphasized that elimination of both pathways resulted in almost complete loss of febrile and cold-evoked thermogenesis.

Possible neurotransmitter/modulators in the orexin neurons for PGE_2-induced fever and cold defence

The pharmacological experiment indicated the possible involvement of glutamate receptors in PGE_2-induced thermogenesis. However, this experiment had 3 major limitations. First, excitation of the orexin neurons would be indirect because there is no report showing existence of EP3 receptors on the orexin neurons. Even if PGE_2 had been injected into the preoptic area, where EP3 receptors are abundant (Nakamura *et al.*, 2005), as in the experiment shown in Fig. 1, it would then activate several neurons other than the orexin neurons. To specifically excite the orexin neurons, we should use photostimulation of orexin/channelrhodopsin-transgenic mice (Adamantidis *et al.*, 2007). Second limitation was the low solubility of SB334867 in ACSF. We cannot exclude the possible contribution of orexin-1 receptors in PGE_2-induced thermoregulation because PGE_2-induced shivering was attenuated in ORX-KO (Fig. 1). Nevertheless, results from our pharmacological study (Fig. 9) support normal thermogenesis in ORX-KO mice. Third limitation was that relatively large volume used in this experiment (2 times of 2 microliters, icv) might cause unspecific effects. However, we compared the effect of antagonists (SB334867, OX2 29, AP5, CNQX) with that of the same volume of vehicle (ACSF). In addition, we confirmed in our preliminary experiment that injection of ACSF plus ACSF did not cause any effect on body temperature and that injection of PGE_2 alone (without pretreatment) induced a similar increase of body temperature as injection of ACSF plus PGE_2. Therefore, we believe that our conclusion (glutamate receptor antagonists but not orexin receptor antagonists were effective) will not change when smaller volume would be used.

Although we cannot exclude the possible contribution of other co-localising substances, such as dynorphin (Chou *et al.*, 2001), galanin (Hakansson *et al.*, 1999), and nitric oxide (Cheng *et al.*, 2003) in PGE_2-induced thermogenesis and cold defence, a possible contribution of glutamate is well supported in the literature. Microinjection of glutamate receptor antagonists into the raphe pallidus inhibited the activation of BAT sympathetic nerves that were evoked by stimulation of DMH/DHA (Cao & Morrison,

2006), by PGE2 (Madden & Morrison, 2003), and by cold exposure (Nakamura & Morrison, 2007). Microinjection of a non-selective glutamate receptor antagonist, kynurenate, into the DMH/DHA inhibited BAT sympathetic activation evoked by PGE_2 into the preoptic area (Madden & Morrison, 2004). On the other hand, dynorphin (Handler *et al.*, 1994) and nitric oxide (Steiner *et al.*, 2002) within the brain have been suggested as thermolytic. Nevertheless, it should be clarified whether glutamate in the orexin neurons actually contribute to the thermogenic responses.

References

Abrahamson EE, Leak RK & Moore RY. (2001). The suprachiasmatic nucleus projects to posterior hypothalamic arousal systems. *Neuroreport* **12,** 435-440.

Adamantidis AR, Zhang F, Aravanis AM, Deisseroth K & de Lecea L. (2007). Neural substrates of awakening probed with optogenetic control of hypocretin neurons. *Nature* **450,** 420-424.

Arrigoni E, Mochizuki T & Scammell TE. (2010). Activation of the basal forebrain by the orexin/hypocretin neurons. *Acta Physiol* **198,** 223-235.

Berthoud H-R, Patterson LM, Sutton GM, Morrison C & Zheng H. (2005). Orexin inputs to caudal raphé neurons involved in thermal, cardiovascular, and gastrointestinal regulation. *Histochem Cell Biol* **123,** 147-156.

Cano G, Passerin AM, Schiltz JC, Card JP, Morrison SF & Sved AF. (2003). Anatomical substrates for the central control of sympathetic outflow to interscapular adipose tissue during cold exposure. *J Comp Neurol* **460,** 303-326.

Cao W-H & Morrison SF. (2006). Glutamate receptors in the raphe pallidus mediate brown adipose tissue thermogenesis evoked by activation of dorsomedial hypothalamic neurons. *Neuropharmacol* **51,** 426-437.

Chemelli RM, Willie JT, Sinton CM, Elmquist JK, Scammell T, Lee C, Richardson JA, Williams SC, Xiong Y, Kisanuki Y, Fitch TE, Nakazato M, Hammer RE, Saper CB & Yanagisawa M. (1999). Narcolepsy in orexin knockout mice: molecular genetics of sleep regulation. *Cell* **98,** 437-451.

Cheng SB, Kuchiiwa S, Gao HZ, Kuchiiwa T & Nakagawa S. (2003). Morphological study of orexin neurons in the hypothalamus of the Long-Evans rat, with special reference to co-expression of orexin and NADPH-diaphorase or nitric oxide synthase activities. *Neurosci Res* **46,** 53-62.

Chou TC, Lee CE, Lu J, Elmquist JK, Hara J, Willie JT, Beuckmann CT, Chemelli RM, Sakurai T, Yanagisawa M, Saper CB & Scammell TE. (2001). Orexin (hypocretin) neurons contain dynorphin. *J Neurosci* **21,** RC168: 161-166.

Conte WL, Kamishina H & Reep RL. (2009). Multiple neuroanatomical tract-tracing using fluorescent Alexa Fluor conjugates of cholera toxin subunit B in rats. *Nature Protocols* **4,** 1157-1166.

Deng B-S, Nakamura A, Zhang W, Yanagisawa M, Fukuda Y & Kuwaki T. (2007). Contribution of orexin in hypercapnic chemoreflex: Evidence from genetic and

pharmacological disruption and supplementation studies in mice. *J Appl Physiol* **103,** 1772-1779.

DiMicco JA & Zaretsky DV. (2007). The dorsomedial hypothalamus: a new player in thermoregulation. *Am J Physiol Regul Integr Comp Physiol* **292,** R47-R63.

Elias CF, Saper CB, Maratos-Flier E, Tritos NA, Lee C, Kelly J, Tatro JB, Hoffman GE, Ollmann MM, Barsh GS, Sakurai T, Yanagisawa M & Elmquist JK. (1998). Chemically defined projections linking the mediobasal hypothalamus and the lateral hypothalamic area. *J Comp Neurol* **402,** 442-459.

Estabrooke IV, McCarthy MT, Ko E, Chou TC, Chemelli RM, Yanagisawa M, Saper CB & Scammell TE. (2001). Fos expression in orexin neurons varies with behavioral state. *J Neurosci* **21,** 1656-1662.

Fadel J, Bubser M & Deutch AY. (2002). Differential activation of orexin neurons by antipsychotic drugs associated with weight gain. *J Neurosci* **22,** 6742-6746.

Hakansson M, de Lecea L, Sutcliffe JG, Yanagisawa M & Meister B. (1999). Leptin receptor- and STAT3-immunoreactivities in hypocretin/orexin neurones of the lateral hypothalamus. *J Neuroendocrinol* **11,** 653-663.

Handler CM, Piliero TC, Geller EB & Adler MW. (1994). Effect of ambient temperature on the ability of *mu*-, *kappa*- and *delta*-selective opioid agonists to modulate thermoregulatory mechanisms in the rat. *J Pharmacol Exp Ther* **268,** 847-855.

Hara J, Beuckmann CT, Nambu T, Willie JT, Chemelli RM, Sinton CM, Sugiyama F, Yagami K, Goto K, Yanagisawa M & Sakurai T. (2001). Genetic ablation of orexin neurons in mice results in narcolepsy, hypophagia, and obesity. *Neuron* **30,** 345-354.

Harris GC, Wimmer M & Aston-Jones G. (2005). A role for lateral hypothalamic orexin neurons in reward seeking. *Nature* **437,** 556-559.

Kayaba Y, Nakamura A, Kasuya Y, Ohuchi T, Yanagisawa M, Komuro I, Fukuda Y & Kuwaki T. (2003). Attenuated defense response and low basal blood pressure in orexin knockout mice. *Am J Physiol Regul Integr Comp Physiol* **285,** R581-R593.

Li Y, Gao X-B, Sakurai T & Pol ANvd. (2002). Hypocretin/orexin excites hypocretin neurons via a local glutamate neuron—a potential mechanism for orchestrating the hypothalamic arousal system. *Neuron* **36,** 1169-1181.

Madden CJ & Morrison SF. (2003). Excitatory amino acid receptor activation in the raphe pallidus area mediates prostaglandin-evoked thermogenesis. *Neurosci* **122,** 5-15.

Madden CJ & Morrison SF. (2004). Excitatory amino acid receptors in the dorsomedial hypothalamus mediate prostaglandin-evoked thermogenesis in brown adipose tissue. *Am J Physiol Regul Integr Comp Physiol* **286,** R320-R325.

McAllen RM, Tanaka M, Ootsuka Y & McKinley MJ. (2010). Multiple thermoregulatory effectors with independent central controls. *Eur J Appl Physiol* **109,** 27-33.

Mileykovskiy BY, Kiyashchenko LI & Siegel JM. (2005). Behavioral correlates of activity in identified hypocretin/orexin neurons. *Neuron* **46,** 787-798.

Morrison SF. (2011). Central neural pathways for thermoregulatory cold defense. *J Appl Physiol* **110,** 1137-1149.

Morrison SF & Nakamura K. (2011). Central neural pathways for thermoregulation. *Front Biosci* **16,** 74-104.

Nakamura K. (2011). Central circuitries for body temperature regulation and fever. *Am J Physiol Regul Integr Comp Physiol* **301,** R1207-R1228.

Nakamura K & Morrison SF. (2007). Central efferent pathways mediating skin cooling-evoked sympathetic thermogenesis in brown adipose tissue. *Am J Physiol Regul Integr Comp Physiol* **292,** R127-R136.

Nakamura K & Morrison SF. (2011). Central efferent pathways for cold-defensive and febrile shivering. *J Physiol (London)* **589,** 3641-3658.

Nakamura Y, Nakamura K, Matsumura K, Kobayashi S, Kaneko T & Morrison SF. (2005). Direct pyrogenic input from prostaglandin EP3 receptor-expressing preoptic neurons to the dorsomedial hypothalamus. *Eur J Neurosci* **22,** 3137-3146.

Nambu T, Sakurai T, Mizukami K, Hosoya Y, Yanagisawa M & Goto K. (1999). Distribution of orexin neurons in the adult rat brain. *Brain Res* **827,** 243-260.

Oldfield BJ, GilesME, Watson A, Anderson C, Colvill LM & Mckinley MJ. (2002). The neurochemical characterisation of hypothalamic pathways projecting polysynaptically to brown adipose tissue in the rat. *Neuroscience* **110,** 515-526.

Paxinos G & Franklin KBJ. (2001). *The Mouse Brain in Stereotaxic Coordinates Second Edition*. Academic Press, Tokyo.

Peyron C, Tighe DK, van den Pol AN, de Lecea L, Heller HC, Sutcliffe JG & Kilduff TS. (1998). Neurons containing hypocretin (orexin) project to multiple neuronal systems. *J Neurosci* **18,** 9996-10015.

Rathner J, Madden C & Morrison S. (2008). Central pathway for spontaneous and

prostaglandin E2-evoked cutaneous vasoconstriction. *Am J Physiol Regul Integr Comp Physiol* **295,** R343-R354.

Rosin DL, Weston MC, Sevigny CP, Stornetta RL & Guyenet PG. (2003). Hypothalamic orexin (hypocretin) neurons express vesicular glutamate transporters VGLUT1 or VGLUT2. *J Comp Neurol* **465,** 593-603.

Rusyniak DE, Zaretskya DV, Zaretskaiaa MV & DiMiccob JA. (2011). The role of orexin-1 receptors in physiologic responses evoked by microinjection of PgE2 or muscimol into the medial preoptic area. *Neurosci Lett* **498,** 162-166.

Sakurai T. (2007). The neural circuit of orexin (hypocretin): maintaining sleep and wakefulness. *Nat Rev Neurosci* **8,** 171-181.

Sakurai T, Amemiya A, Ishii M, Matsuzaki I, Chemelli RM, Tanaka H, Williams SC, Richarson JA, Kozlowski GP, Wilson S, Arch JR, Buckingham RE, Haynes AC, Carr SA, Annan RS, McNulty DE, Liu WS, Terrett JA, Elshourbagy NA, Bergsma DJ & Yanagisawa M. (1998). Orexins and orexin receptors: a family of hypothalamic neuropeptides and G protein-coupled receptors that regulate feeding behavior. *Cell* **92,** 573-585.

Samuels BC, Zaretsky DV & DiMicco JA. (2004). Dorsomedial hypothalamic sites where disinhibition evokes tachycardia correlate with location of raphe-projecting neurons. *Am J Physiol Regul Integr Comp Physiol* **287,** R472-R478.

Schöne C, Cao ZFH, Apergis-Schoute J, Adamantidis A, Sakurai T & Burdakov D. (2012). Optogenetic probing of fast glutamatergic transmission from hypocretin/orexin to histamine neurons In situ. *J Neurosci* **32,** 12437-12443.

Sellayah D, Bharaj P & Sikder D. (2011). Orexin is required for brown adipose tissue development, differentiation, and function. *Cell Metab* **14,** 478-490.

Steiner AA, Antunes-Rodrigues J, McCann SM & Branco LG. (2002). Antipyretic role of the NO-cGMP pathway in the anteroventral preoptic region of the rat brain. *Am J Physiol Regul Integr Comp Physiol* **282,** R584-R593.

Sunanaga J, Deng BS, Zhang W, Kanmura Y & Kuwaki T. (2009). CO_2 activates orexin-containing neurons in mice. *Respir Physiol Neurobiol* **166,** 184-186.

Takahashi K, Lin JS & Sakai K. (2008). Neuronal activity of orexin and non-orexin waking-active neurons during wake–sleep states in the mouse. *Neuroscience* **153,** 860-870.

Terada J, Nakamura A, Zhang W, Yanagisawa M, Kuriyama T, Fukuda Y & Kuwaki T.

(2008). Ventilatory long-term facilitation in mice can be observed both during sleep and wake periods and depends on orexin. *J Appl Physiol* **104,** 499-507.

Torrealba F, Yanagisawa M & Saper CB. (2003). Colocalization of orexin A and glutamate immunoreactivity in axon terminals in the tuberomammillary nucleus in rats. *Neuroscience* **119,** 1033-1044.

Toyama S, Sakurai T, Tatsumi K & Kuwaki T. (2009). Attenuated phrenic long-term facilitation in orexin neuron-ablated mice. *Respir Physiol Neurobiol* **168,** 295-302.

Tupone D, Madden CJ, Cano G & Morrison SF. (2011). An orexinergic projection from perifornical hypothalamus to raphe pallidus increases rat brown adipose tissue thermogenesis. *J Neurosci* **31,** 15944-15955.

Vinkers CH, Groenink L, van Bogaert MJV, Westphal KGC, Kalkman CJ, van Oorschot R, Oosting RS, Olivier B & Korte SM. (2009). Stress-induced hyperthermia and infection-induced fever: Two of a kind? *Physiol Behav* **98,** 37-43.

Watanabe S, Kuwaki T, Yanagisawa M, Fukuda Y & Shimoyama M. (2005). Persistent pain and stress activate pain-inhibitory orexin pathways. *Neuroreport* **16,** 5-8.

Yamanaka A, Beuckmann CT, Willie JT, Hara J, Tsujino N, Mieda M, Tominaga M, Yagami K, Sugiyama F, Goto K, Yanagisawa M & Sakurai T. (2003). Hypothalamic orexin neurons regulate arousal according to energy balance in mice. *Neuron* **38,** 701-713.

Yoshida K, Li X, Cano G, Lazarus M & Saper CB. (2009). Parallel preoptic pathways for thermoregulation. *J Neurosci* **29,** 11954-11964.

Zhang W, Sakurai T, Fukuda Y & Kuwaki T. (2006). Orexin neuron-mediated skeletal muscle vasodilation and shift of baroreflex during defense response in mice. *Am J Physiol Regul Integr Comp Physiol* **290,** R1654-R1663.

Zhang W, Sunanaga J, Takahashi Y, Mori T, Sakurai T, Kanmura Y & Kuwaki T. (2010). Orexin neurons are indispensable for stress-induced thermogenesis in mice. *J Physiol (London)* **588,** 4117-4129.

Zhang W, Zhang N, Sakurai T & Kuwaki T. (2009). Orexin neurons in the hypothalamus mediate cardiorespiratory responses induced by disinhibition of the amygdala and bed nucleus of the stria terminalis. *Brain Res* **1262,** 25-37.

Acknowledgements

We thank Ms. Tae Tabuchi, Hitomi Kasuga, and Miki Sakoda for their technical assistance. We thank Prof. Akihide Tanimoto at Department of Molecular and Cellular Pathology, Kagoshima University Graduate School of Medical and Dental Sciences, for his help in H.E. staining of the BAT tissue. We also thank Joint Research Laboratory, Kagoshima University Graduate School of Medical and Dental Sciences, for the use of their facilities. Part of the work was supported by the Grants-in Aid for Scientific Research from the Ministry of Education, Science, Culture and Sports, Japan.

Author contributions

Conception and design: T.K.

Data collection: Y.T., W.Z., K.S., C.K., A.M., J.S. and Y.Ko.

Analysis and interpretation: Y.T., W.Z., K.S., T.S., Y.Ka. and T.K.

Article drafting and revisions: Y.T., W.Z. and T.K.

All authors approved the final version of the manuscript

Figure Legends

Figure 1. Effect of microinjections of PGE_2 into the medial preoptic area on body temperature and the electromyogram in the mice of the 4 genotypes. In chloralose (80 $mg \cdot kg^{-1}$)/urethane (800 $mg \cdot kg^{-1}$)-anaesthetised mice, ACSF (20 nL) and PGE_2 (1 $mg \cdot mL^{-1}$ in ACSF) were sequentially microinjected into the medial preoptic area (MPO) (D, E). Time-related changes in brown adipose tissue (BAT) temperature, rectal temperature, and nuchal EMG (a measure of shivering) are shown in A, B, and C, respectively, and the changes expressed as the area under the curve above the baseline in them for 70 min are summarized in A', B', and C', respectively. Data are presented as mean ± SEM of orexin-knockout mice (ORX-KO, n = 6), orexin neuron-ablated mice (ORX-AB, n = 6), and their corresponding wild-type littermates (WT_{KO}, n = 4 and WT_{AB}, n = 5). (E) Summary for injected sites. Left-side shows dye-distribution in WT_{KO} and WT_{AB} mice and right-side shows that of ORX-KO and ORX-AB mice. In the actual experiment, drugs and dye were injected into unilateral MPO. * $p < 0.05$ compared with baseline values before injection (Bonferroni's post hoc test). n.s., not significant. ac, anterior commissure; MnPO, median preoptic area.

Figure 2. Effect of administration of PGE2 into the lateral ventricle on abdominal temperature in freely moving mice with indwelling telemeters of 4 genotypes. ACSF (2 µL) or PGE_2 (1 $mg \cdot mL^{-1}$ in ACSF) were administered through a cerebroventricular cannula in a random order with an intermission of at least 2 days. Abdominal temperature was continuously monitored by a telemetric system. Time-related changes (A) and the changes expressed as the area under the curve above the baseline for 100 min (B) are shown. Data are presented as mean ± SEM of orexin-knockout mice (ORX-KO, n = 8 for PGE_2 and n = 6 for ACSF), orexin neuron-ablated mice (ORX-AB, n = 8 for PGE_2 and n = 5 for ACSF), and their corresponding wild-type littermates (WT_{KO}, n = 8 for PGE_2 and n = 6 for ACSF and WT_{AB}, n = 7 for PGE_2 and n = 6 for ACSF). * $p < 0.05$ compared with baseline value before injection (Bonferroni's post hoc test). n.s., not significant.

Figure 3. Effect of cold exposure on abdominal temperature and locomotor activity in freely moving mice with indwelling telemeters of the 4 genotypes. Mice were exposed to a cold environment (5°C) for 4 h while abdominal temperature and locomotor

activity were continuously monitored by a telemetric system. When the animal's body temperature decreased below 30°C, cold exposure was terminated and the animal was immediately warmed up with a heating lamp. Time-related changes in abdominal temperature (A) and locomotor activity (B) are shown. The thin grey lines indicate the data from an individual animal, and the thick black lines are the mean ± SEM (n = 5 in each group) of orexin-knockout mice (ORX-KO), orexin neuron-ablated mice (ORX-AB), and their corresponding wild-type littermates (WT_{KO} and WT_{AB}). Note that only 1 mouse out of 5 ORX-AB mice tolerated the 4 h of cold exposure. Insets are the changes in the abdominal temperature and locomotor activity expressed as the area under the curve (AUC) above the baseline. AUC was calculated for only 60 min during the initial part of the cold exposure because of the endpoint in some ORX-AB mice. * $p < 0.05$ compared with baseline value before cold exposure (Bonferroni's post hoc test). n.s., not significant.

Figure 4. Effect of heat exposure on abdominal temperature and locomotor activity in freely moving mice with indwelling telemeters of the 4 genotypes. Mice were exposed to a hot environment (39°C) for 1 h while abdominal temperature and locomotor activity were continuously monitored by a telemetric system. Data are presented as mean ± SEM of orexin-knockout mice (ORX-KO, n = 5), orexin neuron-ablated mice (ORX-AB, n = 5), and their corresponding wild-type littermates (WT_{KO}, n = 4 and WT_{AB}, n = 4). Insets are the changes in the abdominal temperature and locomotor activity expressed as the area under the curve above the baseline calculated for 60 min of the heat exposure. * $p < 0.05$ compared with baseline values before heat exposure (Bonferroni's post hoc test). n.s., not significant.

Figure 5. Immunohistochemical evidence for the activation of orexin neurons by the administration of PGE_2 into the lateral ventricle. (A and B) Representative photographs of double immunostaining for orexin and c-fos in the hypothalamus of wild-type (WT) mice sampled 2 h after the administration of ACSF (A) or PGE_2 (B) into the lateral ventricle. Orexin is stained in red, and c-fos is stained in green. Yellow designates cells stained for both orexin and c-fos. Filled triangles indicate double-stained cells, and open triangles indicate orexin-containing but not c-fos expressing cells. Arrows

indicate c-fos in non-orexin cells. (C and D) Representative photographs of immunostaining for c-fos in the hypothalamus of orexin-knockout (KO) mice that carries the orexin neuron-specific expression of green fluorescent protein (KO;GFP+). Brains were sampled 2 h after the administration of ACSF (C) or PGE_2 (D) into the lateral ventricle. c-fos is stained in red. Yellow designates cells that possess GFP and are stained for c-fos. Filled triangles indicate double-labelled cells, and open triangles indicate GFP-containing but not c-fos expressing cells. Arrows indicate c-fos in non-orexin cells. Bar = 100 μm. In (A)-(D), the fornix was indicated in a dashed line. (E) Schematic drawing of a coronal section of the mouse brain showing structure of the hypothalamus. Two rectangles denote examined area (1020 x 675 μm, each) for medial and lateral parts of the dorsal hypothalamus. Both sides were examined in the actual experiment although only right side windows were depicted for simplicity. DMH, dorsomedial hypothalamus; f, fornix; LHA, lateral hypothalamic area; mt, mammillothalamic tract; PeF, perifornical area. (F and G) Numbers of c-fos-immunopositive cells, orexin (ORX) or GFP-containing cells, and double-labelled cells (c-fos and ORX in WT, and c-fos and GFP in KO) in the medial (F) and lateral (G) part of the hypothalamus. Data are presented as the mean ± SEM (n = 4 in each group) of PGE_2- or ACSF-injected WT mice, KO;GFP+ mice, and orexin neuron-ablated mice (ORX-AB). * $p < 0.05$ vs. ACSF. No orexin-immunopositive cells were detected (n.d.) in ORX-AB mice. Note that c-fos did not increase by PGE_2 in the medial hypothalamus of the ORX-AB mice.

Figure 6. Immunohistochemical evidence for activation of orexin neurons by cold exposure. (A and B) Representative photographs of double immunostaining for orexin and c-fos in the hypothalamus of a naïve wild-type (WT) mouse (A) and of a WT mouse exposed to a cold (5°C) environment for 60 min (B). Orexin is stained in red, and c-fos is stained in green. Yellow designates cells stained for both orexin and c-fos. Filled triangles indicate double-stained cells, and open triangles indicate orexin-containing but not c-fos expressing cells. Arrows indicate c-fos in non-orexin cells. (C and D) Representative photographs of immunostaining for c-fos in the hypothalamus of orexin-knockout (KO) mice that carries the orexin neuron-specific expression of green fluorescent protein (KO;GFP+). Brains were sampled from a naïve mouse (C) and from a mouse exposed to a cold (5°C) environment for 60 min (D). c-fos is stained in red. Yellow designates cells

that possess GFP and are stained for c-fos. Filled triangles indicate double-labelled cells, and open triangles indicate GFP-containing but not c-fos expressing cells. Arrows indicate c-fos in non-orexin cells. Bar = 100 μm. Hypothalamic sections were immunostained for orexin and c-fos, as described in the Methods section and in the legend to Fig. 5. (E and F) The bar graph shows the numbers of c-fos-immunopositive cells, orexin (ORX) or GFP-containing cells, and double-labelled cells (c-fos and ORX in WT, and c-fos and GFP in KO) in the medial (E) and lateral (F) part of the hypothalamus (see Fig. 5E for definition of the medial and lateral part). Data are presented as mean ± SEM (n = 4 in each group) of naïve or cold exposed WT mice, KO;GFP+ mice, and ORX-AB mice. * $p < 0.05$ vs. naïve. No orexin-immunopositive cells were detected (n.d.) in ORX-AB mice. Note that c-fos did not increase by cold exposure in the medial hypothalamus of the ORX-AB mice.

Figure 7. Distribution of retrogradely labelled neurons in the hypothalamus following cholera toxin b subunit injection into the rostral raphe pallidus. Schematic diagrams in A and D show locations of cholera toxin subunit b (CTb)-containing (green circles), orexin-immunoreactive (red circles), and double-labelled (black dots) neurons following CTb injection into the rostral raphe pallidus (RPa) (B and E) of wild-type mice (A-C) and orexin neuron-ablated mice (D-F). Results in 4 animals (1 typical specimen per animal) were plotted on an atlas drawing. C and F show representative photographs in wild-type mice and orexin neuron-ablated mice, respectively. C' shows an example of orexin-immunoreactive nerve terminals (arrow) attaching to the CTb-positive cell found in the dorsal hypothalamic area (DHA) in a wild-type mouse. DMH, dorsomedial hypothalamus; f, fornix; FN, facial nucleus; LHA, lateral hypothalamic area; mt, mammillary tract; PeF, perifornical area; Py, pyramidal tract.

Figure 8. Apparently normal morphology of the brown adipose tissue in mutant mice. Intrascapular brown adipose tissues were excised from euthanasiated animals, thin sectioned in paraffin, and stained with haematoxylin and eosin. No apparent reduction in intracellular lipids was observed in orexin-knockout mice (KO) or orexin neuron-ablated mice (AB) as compared to wild-type mice (WT) (n=4, each). Representative images are shown.

Figure 9. Effect of orexin receptor-antagonists (SB334867 and OX2 29) and glutamate receptor-antagonists [D-(-)-2-amino-5-phosphonopentanoic acid (AP5) and 6-cyano-7-nitroquinoxaline-2,3-dione (CNQX)] on PGE_2-induced fever. In chloralose (80 $mg \cdot kg^{-1}$)/urethane (800 $mg \cdot kg^{-1}$)-anaesthetised and artificially ventilated C57BL/6 mice, an orexin receptor antagonist, a glutamate receptor antagonist, or ACSF was administered into the lateral ventricle in a volume of 2 μL at the time indicated by the arrow. After 5 min, PGE_2 (1 $mg \cdot mL^{-1}$, 2 μL) was injected into the same ventricle. Time-related changes in brown adipose tissue (BAT) temperature, rectal temperature, and nuchal electromyogram (EMG, as a measure of shivering) are shown in A, B, and C, respectively, and the changes expressed as the area under the curve above the baseline in them for 90 min are summarized in A', B', and C', respectively. Tested drugs were the following: an orexin receptor-1-specific antagonist, SB334867 (1 mM, n = 6); an orexin receptor-2-specific antagonist, OX2 29 (100 mM, n = 5); a NMDA-selective glutamate receptor antagonist, AP5 (10 mM, n = 8); an AMPA/kainate-selective glutamate receptor antagonist, CNQX (10 mM, n = 6); and ACSF (n = 7). Only 1 drug was tested in each animal. Data are presented as mean ± SEM. * $p < 0.05$ compared with baseline value before injection of antagonist (Bonferroni's post hoc test). † indicates that the values in the 3 groups (ACSF, SB334867, and OX2 29) are significantly different ($p < 0.05$) from the corresponding baseline values. In A'-C', values are compared with that of ACSF group (ANOVA followed by Bonferroni's post hoc test). n.s., not significant. Note that the glutamate receptor antagonists, but not the orexin receptor antagonists, successfully inhibited the PGE_2-induced fever and shivering.

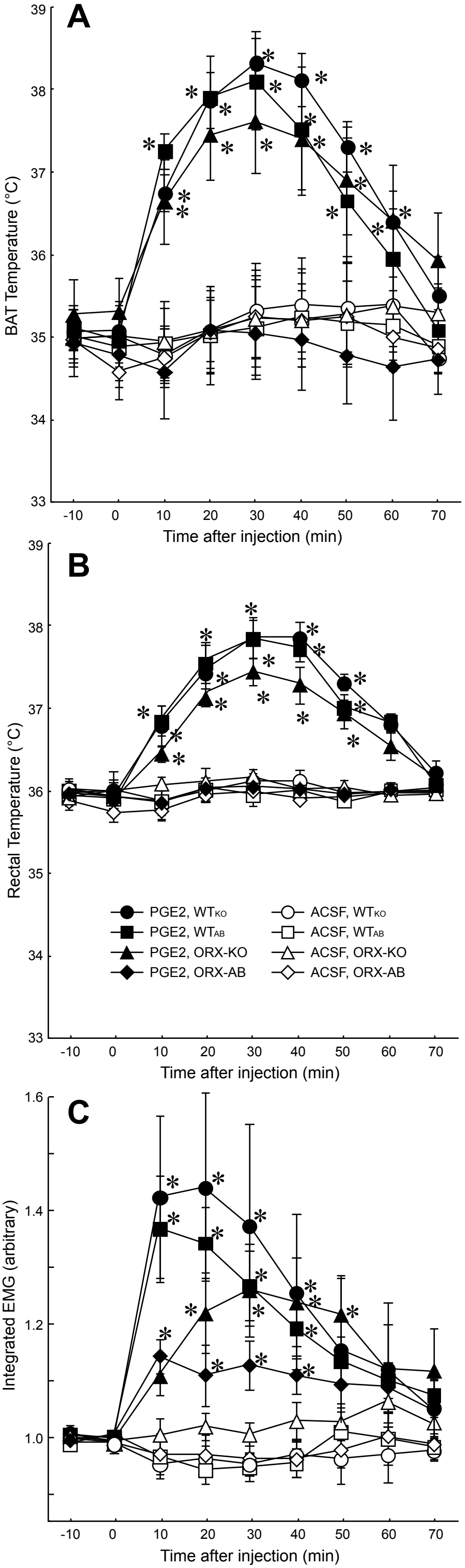
A
BAT Temperature (°C)
Time after injection (min)
B
Rectal Temperature (°C)
PGE2, WTKO
PGE2, WTAB
PGE2, ORX-KO
PGE2, ORX-AB
ACSF, WTKO
ACSF, WTAB
ACSF, ORX-KO
ACSF, ORX-AB
Time after injection (min)
C
Integrated EMG (arbitrary)
Time after injection (min)

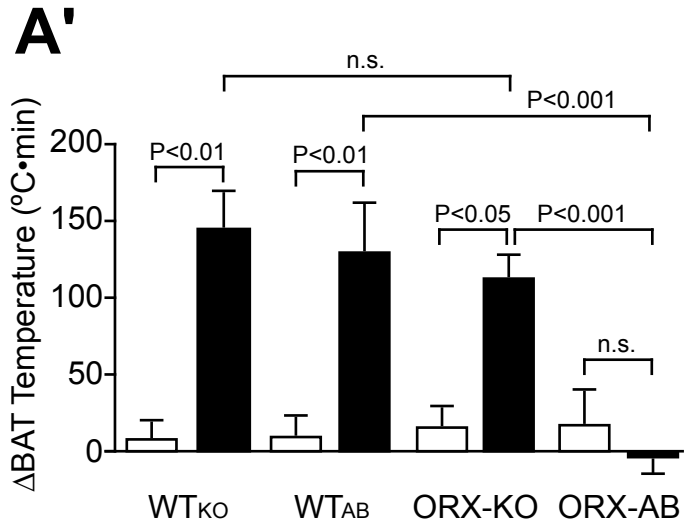
A'
ΔBAT Temperature (ºC•min)
n.s.
P<0.001
P<0.01
P<0.01
P<0.05
P<0.001
n.s.
WTKO
WTAB
ORX-KO
ORX-AB

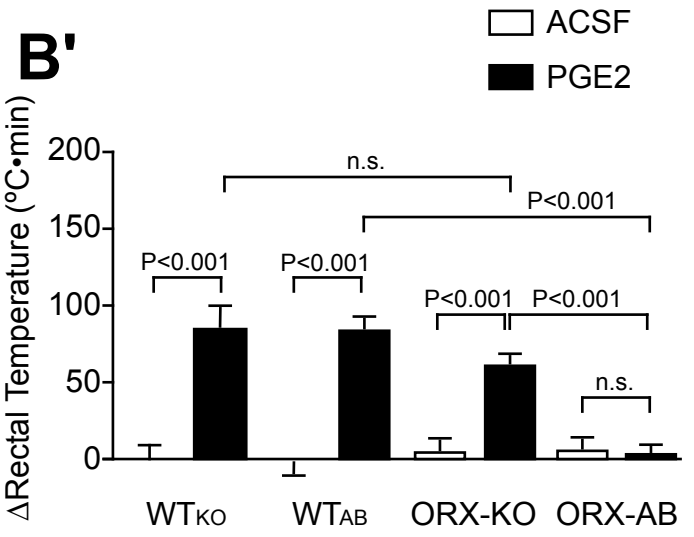
B'
ACSF
PGE2
ΔRectal Temperature (ºC•min)
n.s.
P<0.001
P<0.001
P<0.001
P<0.001
P<0.001
n.s.
WTKO
WTAB
ORX-KO
ORX-AB

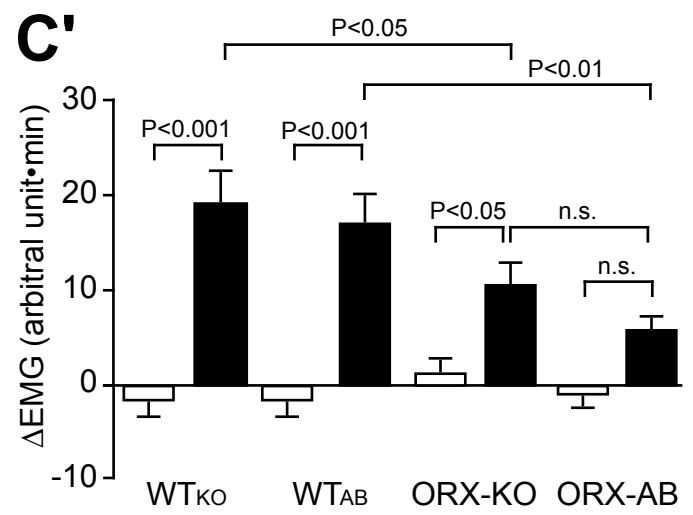
C'
ΔEMG (arbitral unit•min)
P<0.05
P<0.01
P<0.001
P<0.001
P<0.05
n.s.
n.s.
WTKO
WTAB
ORX-KO
ORX-AB

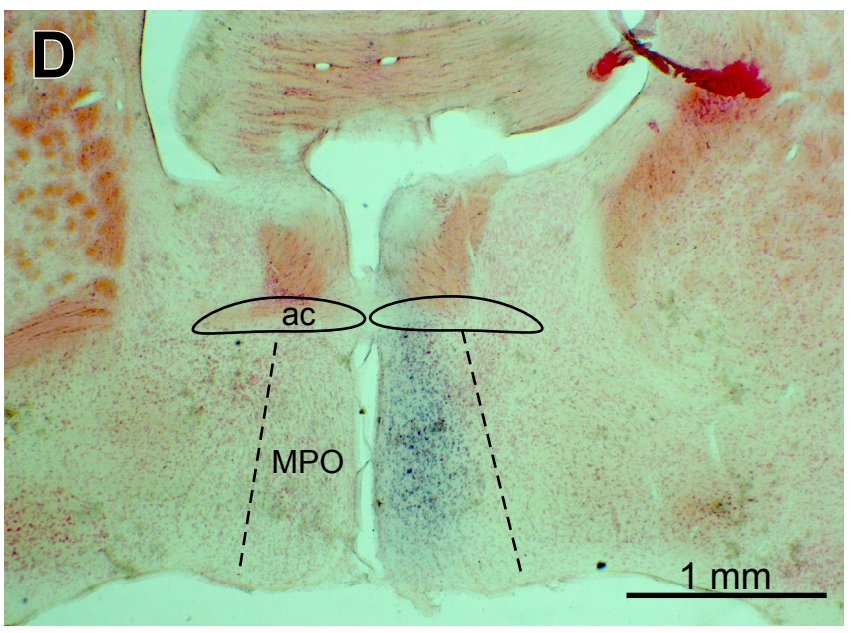
D
ac
MPO
1 mm

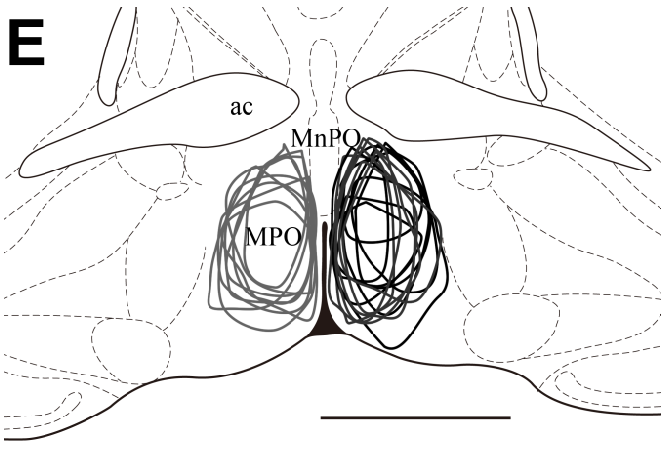
E
ac
MnPO
MPO

Fig. 1

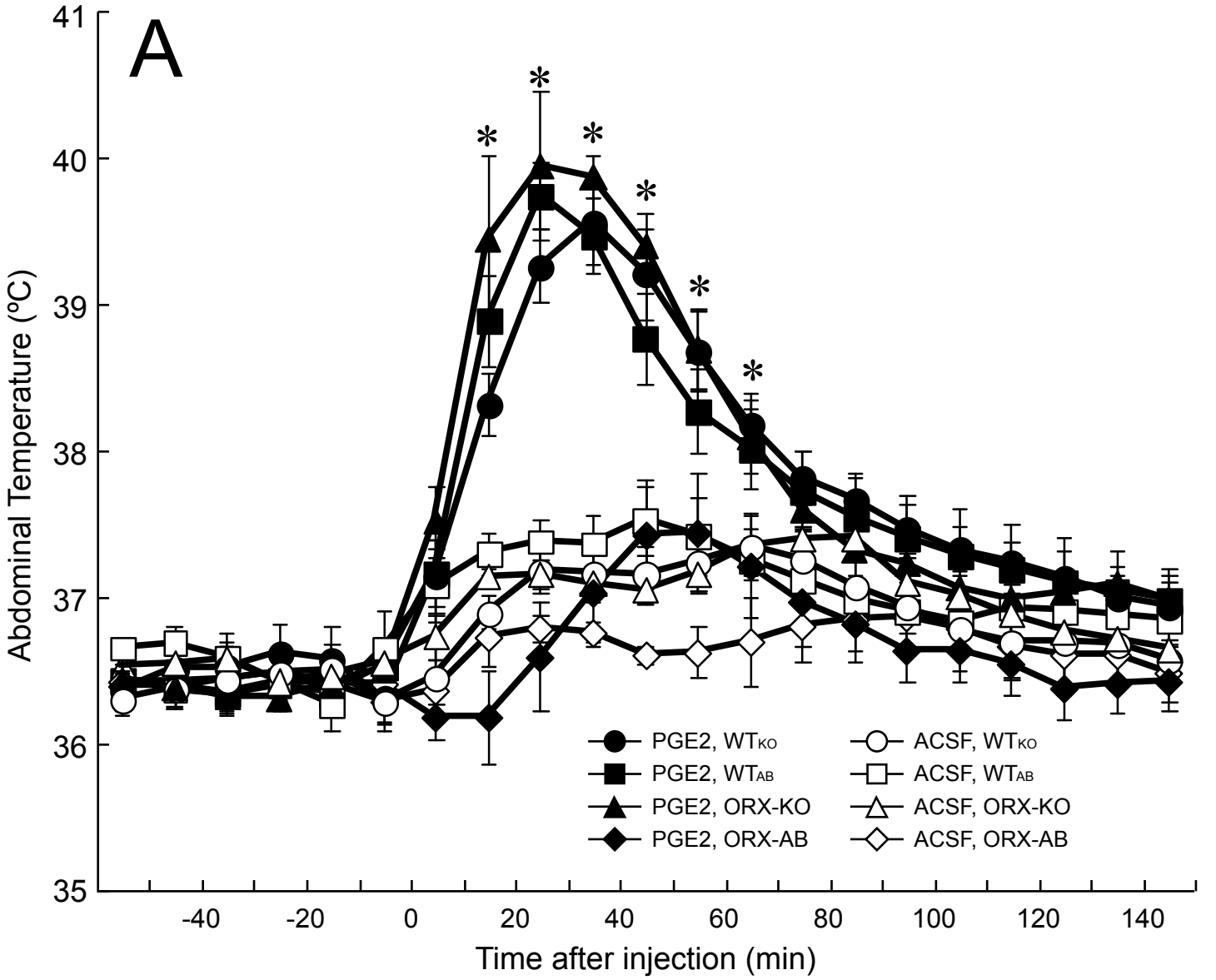
A
Abdominal Temperature (ºC)
Time after injection (min)
PGE2, WTKO
PGE2, WTAB
PGE2, ORX-KO
PGE2, ORX-AB
ACSF, WTKO
ACSF, WTAB
ACSF, ORX-KO
ACSF, ORX-AB

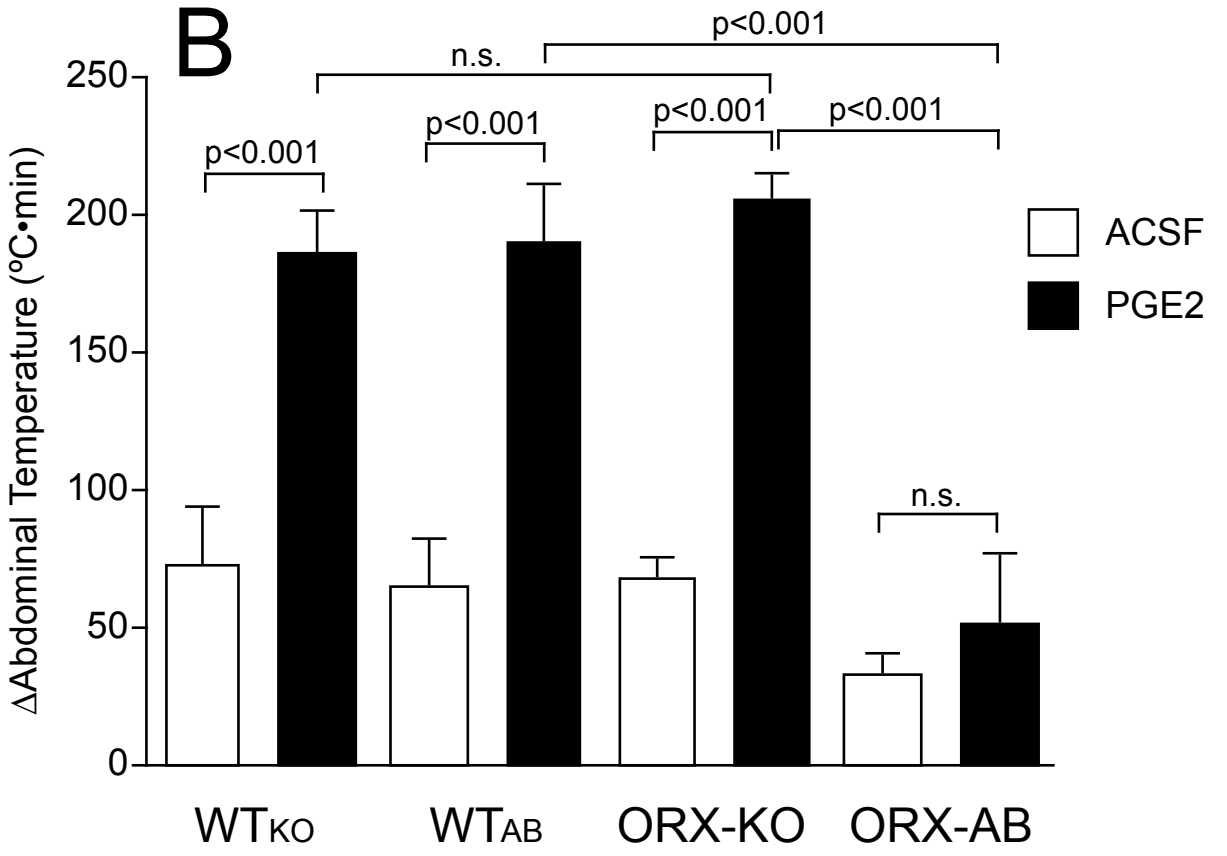
B
ΔAbdominal Temperature (ºC•min)
p<0.001
n.s.
p<0.001
p<0.001
p<0.001
p<0.001
n.s.
ACSF
PGE2
WTKO
WTAB
ORX-KO
ORX-AB

Fig. 2

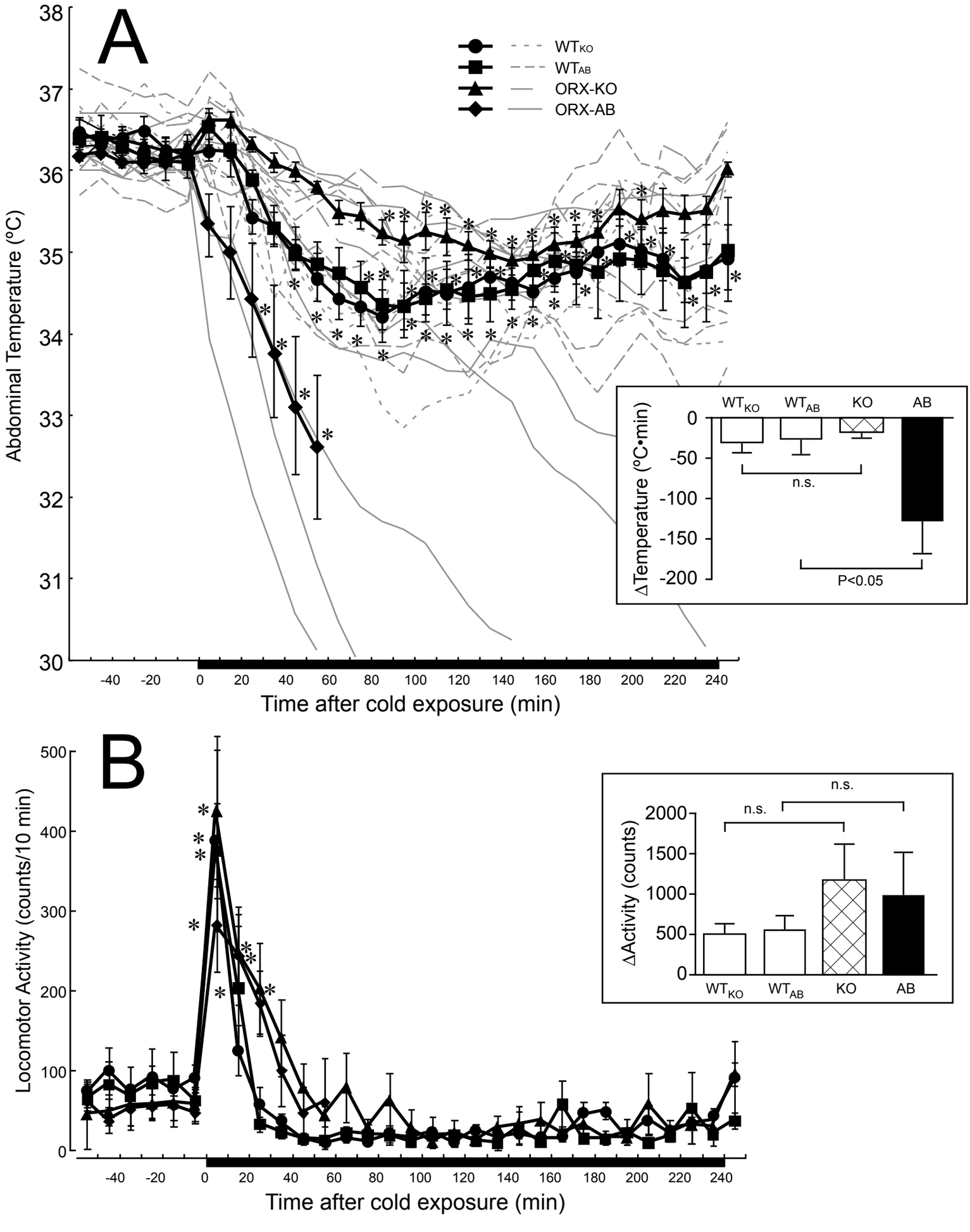
A
WTKO
WTAB
ORX-KO
ORX-AB
Abdominal Temperature (ºC)
Time after cold exposure (min)
ΔTemperature (ºC•min)
WTKO
WTAB
KO
AB
n.s.
P<0.05
B
Locomotor Activity (counts/10 min)
Time after cold exposure (min)
ΔActivity (counts)
n.s.
n.s.
WTKO
WTAB
KO
AB

Fig. 3

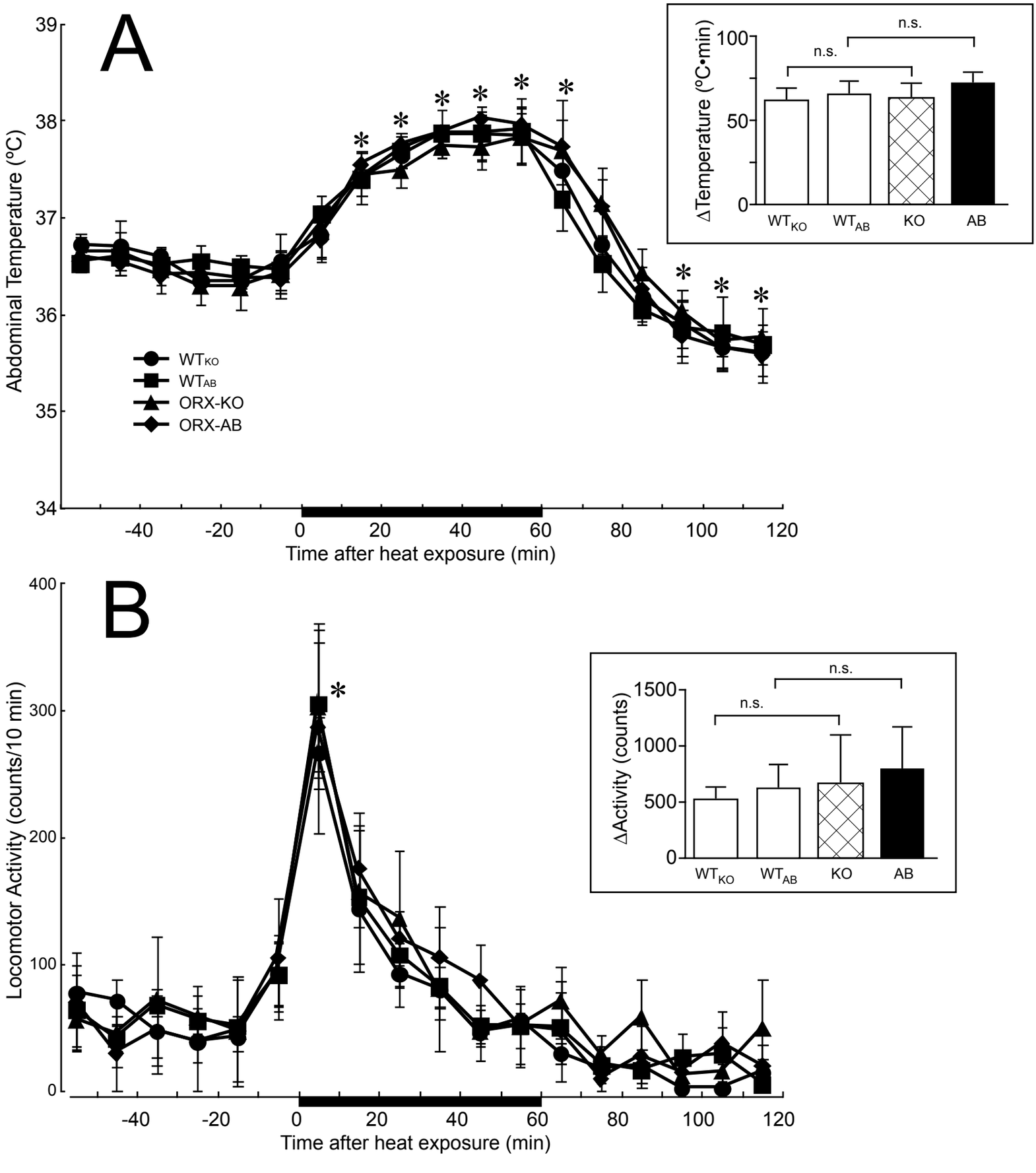
A
Abdominal Temperature (ºC)
Time after heat exposure (min)
WTKO
WTAB
ORX-KO
ORX-AB
ΔTemperature (ºC•min)
n.s.
n.s.
WTKO
WTAB
KO
AB
B
Locomotor Activity (counts/10 min)
Time after heat exposure (min)
ΔActivity (counts)
n.s.
n.s.
WTKO
WTAB
KO
AB

Fig. 4

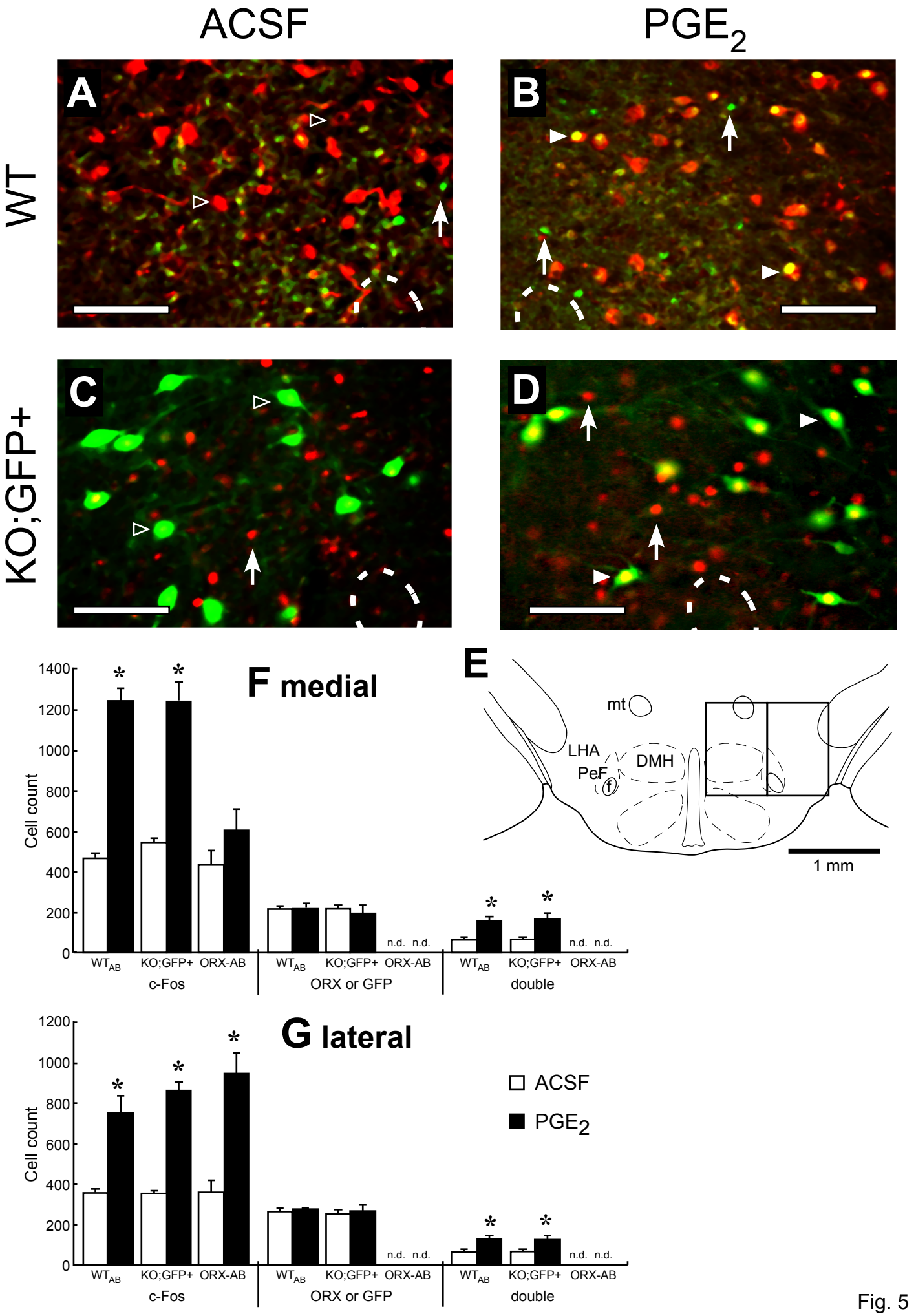
ACSF
PGE2
WT
KO;GFP+
A
B
C
D
E
mt
LHA
PeF
DMH
1 mm
F medial
G lateral
Cell count
1400
1200
1000
800
600
400
200
0
WTAB
KO;GFP+
ORX-AB
c-Fos
ORX or GFP
double
n.d.
ACSF
PGE2

Fig. 5

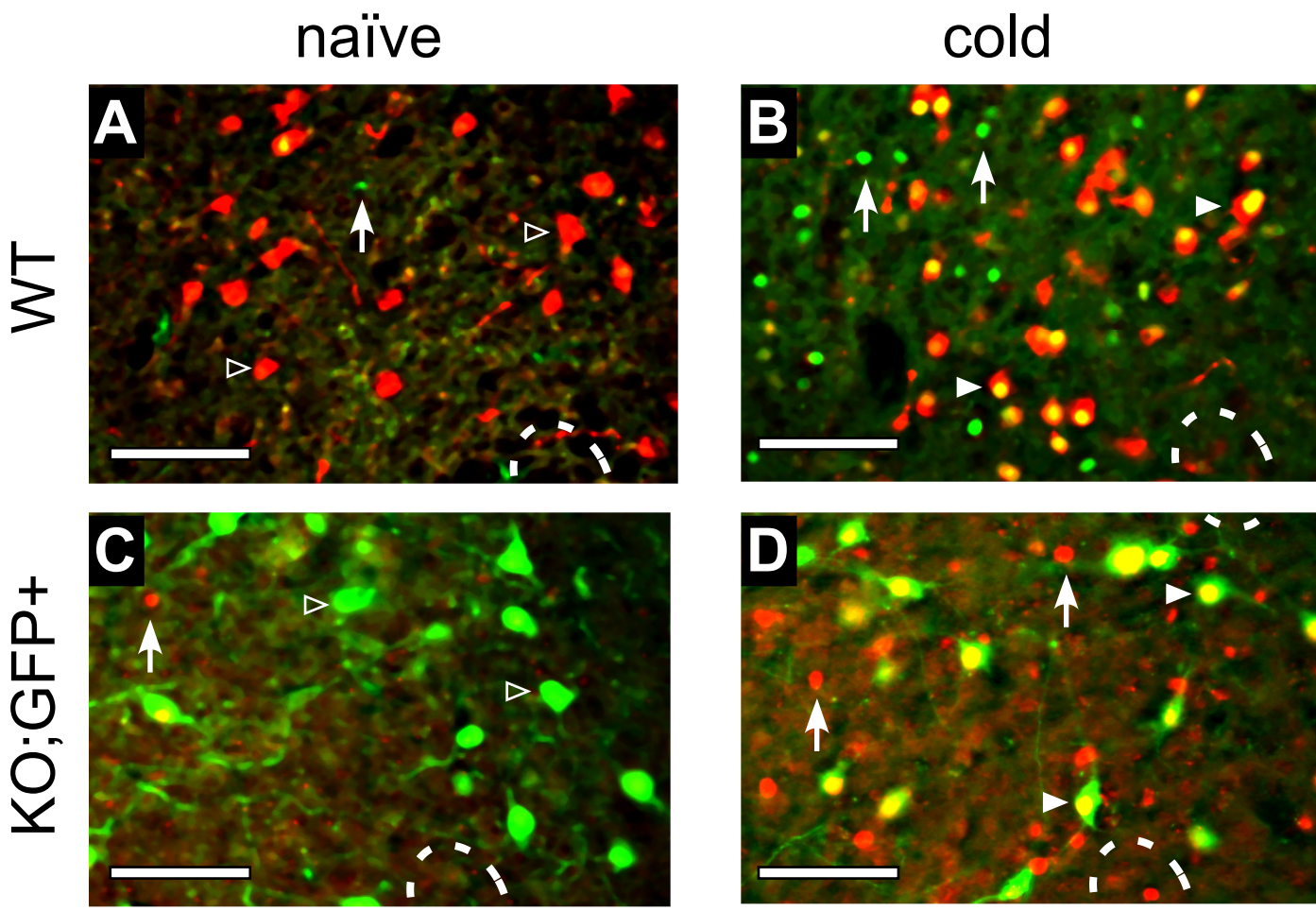
naïve
cold
WT
KO;GFP+
A
B
C
D

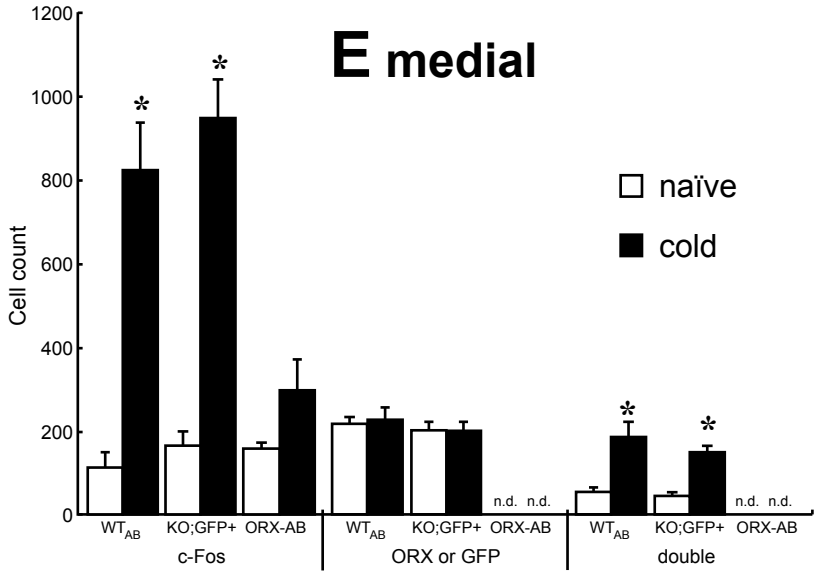
E medial
Cell count
1200
1000
800
600
400
200
0
naïve
cold
WT$_{AB}$
KO;GFP+
ORX-AB
c-Fos
ORX or GFP
double
n.d.

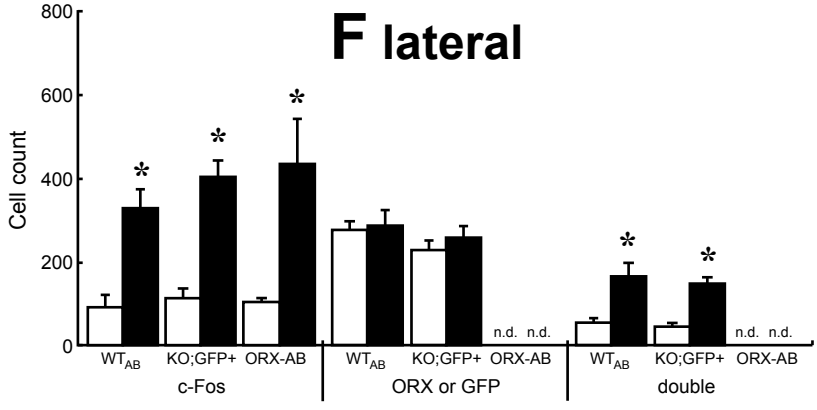
F lateral
Cell count
800
600
400
200
0
WT$_{AB}$
KO;GFP+
ORX-AB
c-Fos
ORX or GFP
double
n.d.

Fig. 6

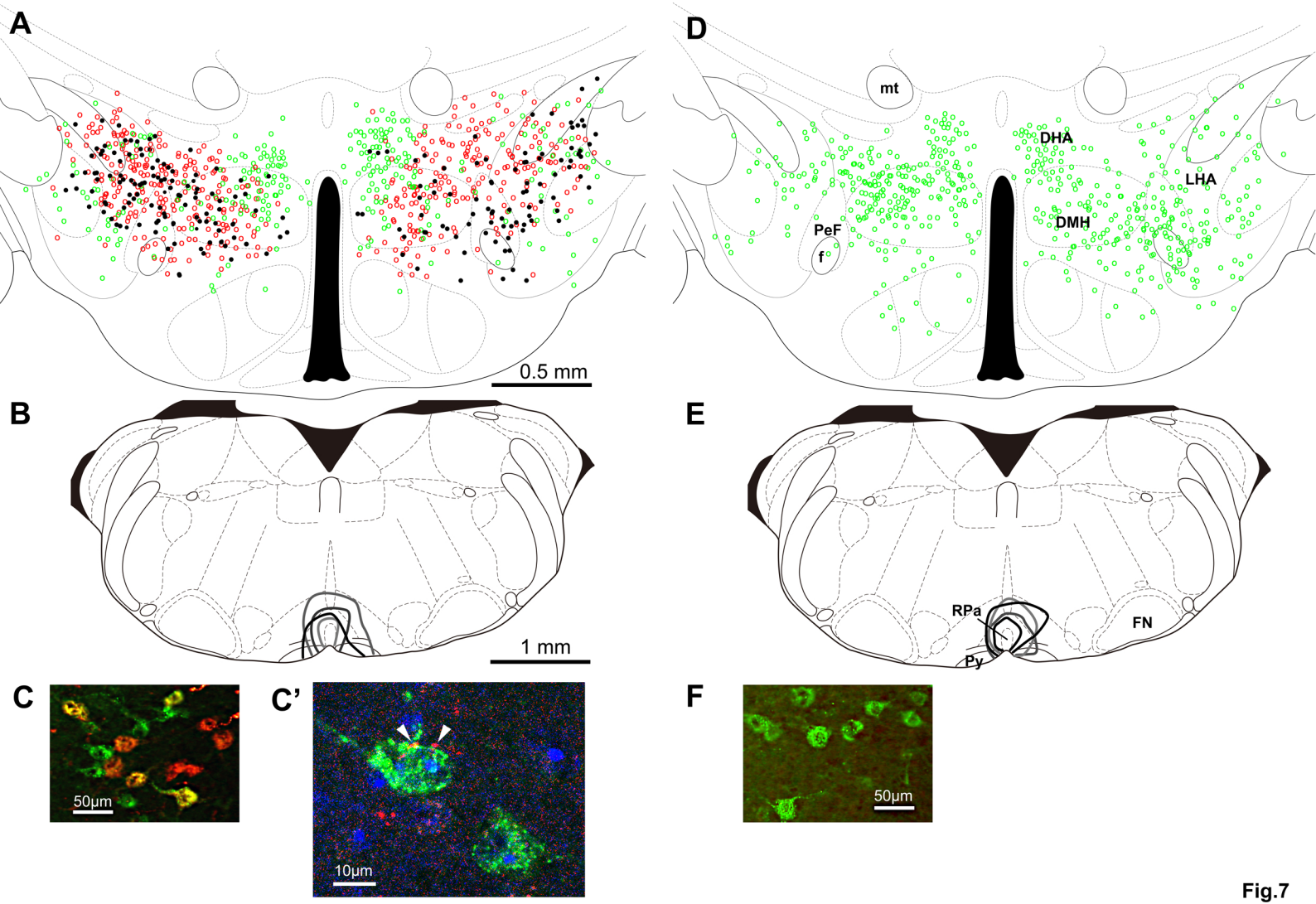

Fig.7

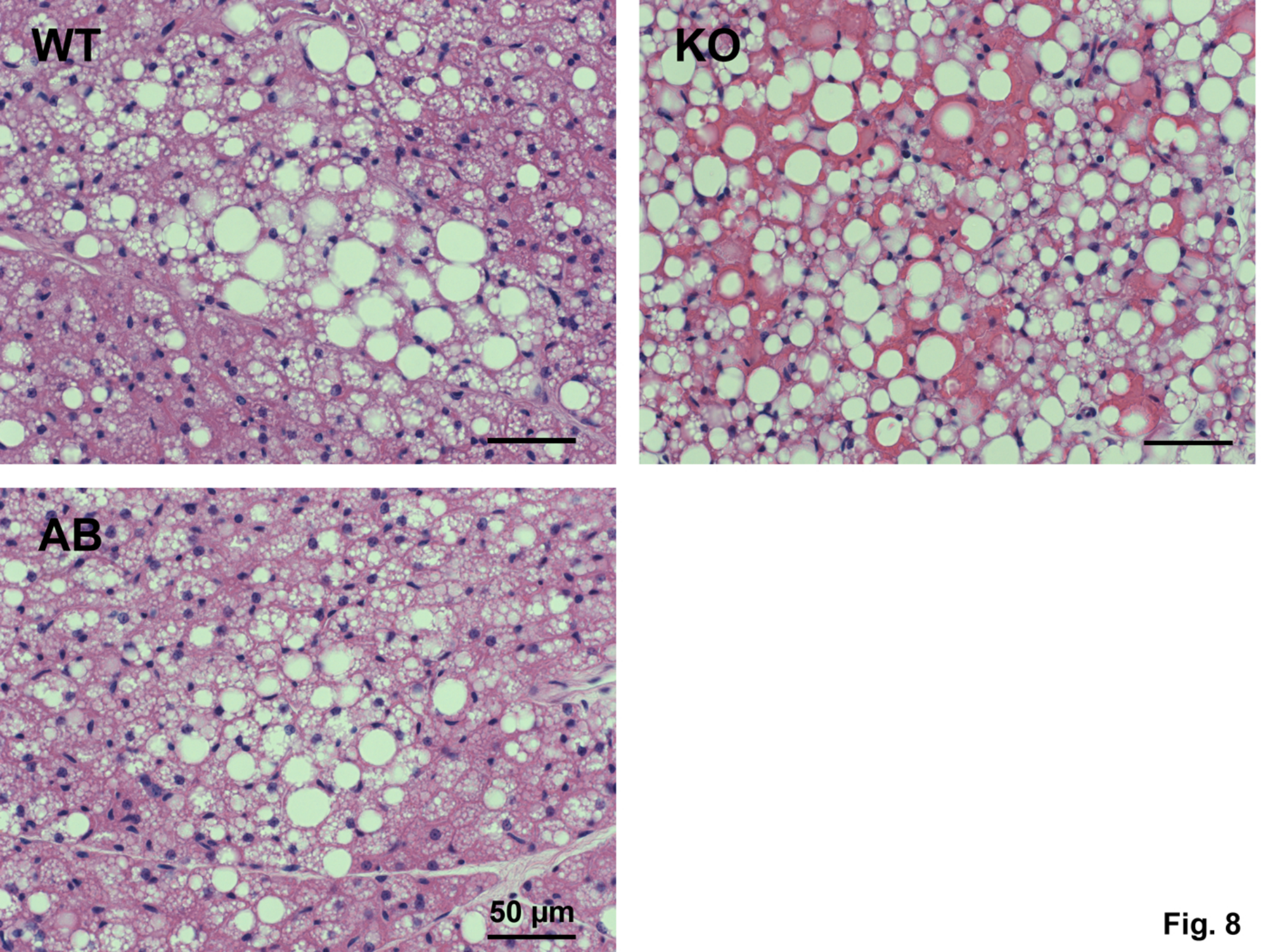

Fig. 8

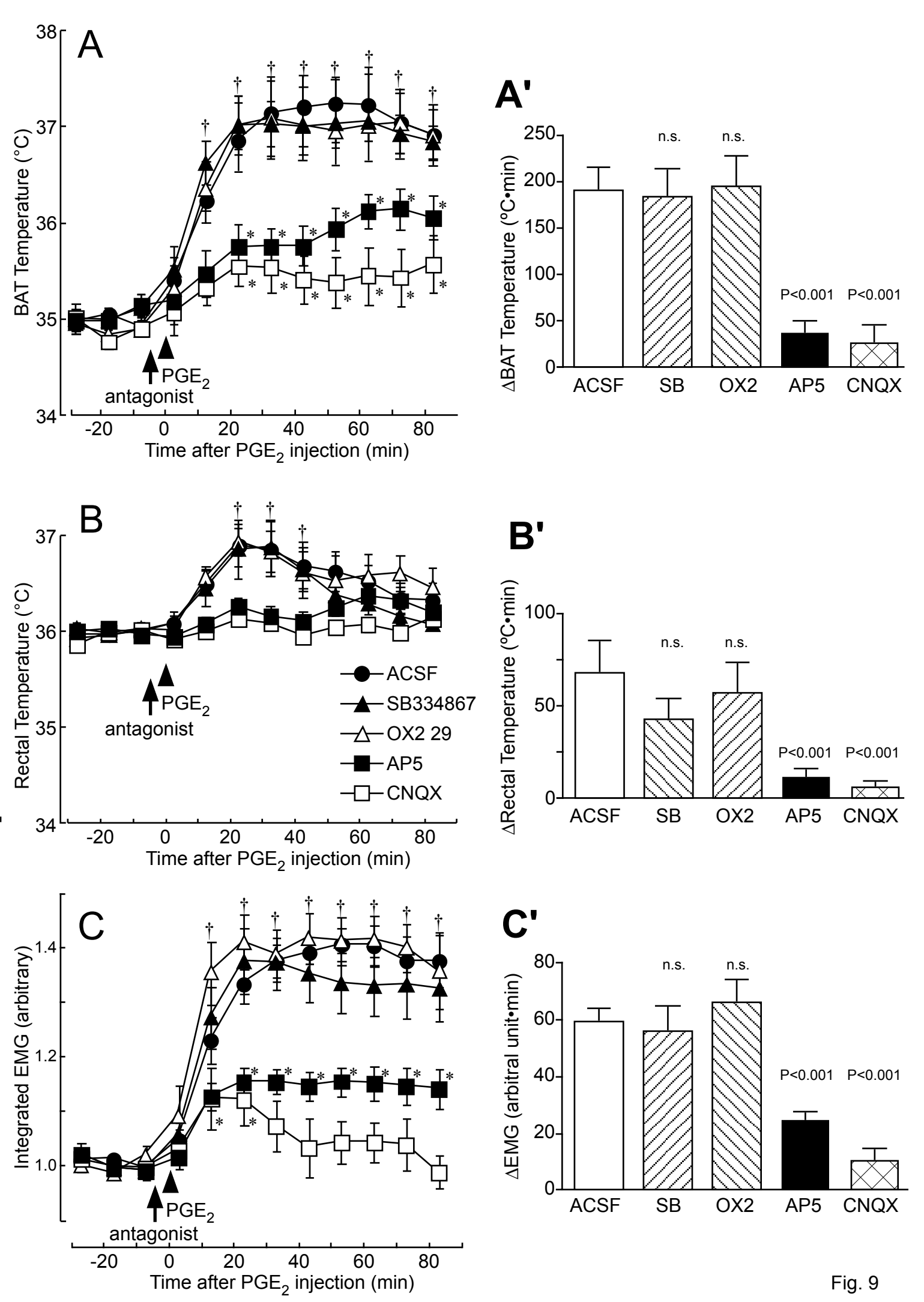
A
BAT Temperature (°C)
38
37
36
35
34
PGE2
antagonist
-20
0
20
40
60
80
Time after PGE2 injection (min)
A'
ΔBAT Temperature (ºC•min)
250
200
150
100
50
0
n.s.
n.s.
P<0.001
P<0.001
ACSF
SB
OX2
AP5
CNQX
B
Rectal Temperature (°C)
37
36
35
34
PGE2
antagonist
ACSF
SB334867
OX2 29
AP5
CNQX
-20
0
20
40
60
80
Time after PGE2 injection (min)
B'
ΔRectal Temperature (ºC•min)
100
50
0
n.s.
n.s.
P<0.001
P<0.001
ACSF
SB
OX2
AP5
CNQX
C
Integrated EMG (arbitrary)
1.4
1.2
1.0
PGE2
antagonist
-20
0
20
40
60
80
Time after PGE2 injection (min)
C'
ΔEMG (arbitral unit•min)
80
60
40
20
0
n.s.
n.s.
P<0.001
P<0.001
ACSF
SB
OX2
AP5
CNQX

Fig. 9